

**SYNTHETIC METHODOLOGIES FOR MOLECULAR IMAGING:  
SYNTHESIS, CYCLIZATION AND IN VITRO BINDING STUDY OF  
DEATH RECEPTOR 5 TARGETED PEPTIDES**

By

**Chenyang Li**

A thesis submitted to The Johns Hopkins University in conformity with the requirements for the  
degree of Master of Science in Engineering

Johns Hopkins University  
Department of Chemical and Biomolecular Engineering

Baltimore, Maryland

June 2018

**Abstract:**

Molecular Imaging (MI) techniques are rapidly developed to achieve precise, early and in-time diagnosis for various disease. Unlike conventional anatomical imaging technique, non-invasive molecular imaging has paved a novel way for disease study and diagnosis on a molecular level in living organism without intervention on its biological process. Molecular imaging can allow clinicians to gain more information on precise localization, visualization of the disease. One strategy to visualize certain disease is to target biomarker on certain cells by designed substrate specific imaging probe.

Tumor necrosis factor (TNF) - related apoptosis-inducing ligand, known as TRAIL, is a promising anticancer ligand that can biologically bind to Death Receptor 5 (DR5). Studies have showed that colorectal cancers have significant DR5 upregulation. Except in oncology, liver fibrosis is also relevant to TRAIL, which is a common chronic liver disease that will lead to liver cirrhosis and hepatocellular carcinoma. Activated hepatic stellate cells (aHSCs) is major abnormal cell types, while studies show aHSCs are associated with elevated expression of death receptors and sensitivity towards TRAIL induced cell death. In this study, five phage-display determined Death Receptor 5 (DR5) targeted peptide has been developed to visualize DR5 and apoptosis simultaneously.

In the initial stage of developing Death Receptor 5 based PET or SPECT imaging agent for living cirrhosis, fluorescent dye, 5-carboxyfluorescent, has been conjugated on the peptide for screening and binding affinity test for developing this PET/SPECT imaging agent.

## Table of Contents

Abstract: .....	ii
Acknowledgement .....	v
List of Tables: .....	vii
List of Figures: .....	vii
Chapter 1: Chemistry of Molecular Imaging .....	viii
Background .....	1
1.1 Molecular Imaging Techniques .....	3
1.1.1 Positron Emission Tomography (PET) .....	3
1.1.2 Single Photon Emission Computed Tomography (SPECT) .....	5
1.1.3 Magnetic Resonance Imaging (MRI) .....	6
1.1.4 CEST MRI imaging .....	7
1.2 PET/SPECT imaging in Central Nervous Disease .....	9
1.3 Prostate Specific Membrane Antigen (PSMA) targeted imaging .....	11
1.4. Chemical Methodology for Radiolabeling .....	13
1.4.1 Halogen Element Radionuclides (F, Br, I) .....	13
1.4.2 Metal Radionuclides (Rb, Ga, In, Cu and Tc) .....	14
1.4.3 Organic Radionuclides (C, N, O) .....	14
1.5 Nanoparticles on Molecular Imaging .....	15
1.5.1 Nanoparticles for Magnetic Resonance Imaging (MRI) .....	15
Chapter 2: Synthesis, Cyclization and In Vitro Binding Study of Death Receptor 5 Targeted Peptides ....	16
2.1 TRAIL-induced apoptosis mechanism .....	17
2.2 TRAIL in Liver and Central Nervous Disease .....	18
2.3 Development of DR5-binding peptides using phage display technique .....	19
2.4 Cyclic peptides and cyclization strategies .....	21
2.5 Labeling Strategies and Methodologies for Peptides .....	22
2.5.1 Halogen-labeled peptide radiopharmaceuticals methods .....	24
2.5.2 <sup>99m</sup> Tc-labeled peptide radiopharmaceuticals method .....	25
2.5.3 Radiometal labeling method .....	26
2.6 Experimental Section .....	28
2.6.1 Materials and methods .....	28
2.7 Result and discussion .....	31
2.8 Future perspectives .....	31

3. Reference .....	32
4. Appendices.....	37

## **Acknowledgement**

First, thank my mother, Jianhong Bai, and my father, Qiangsheng Li for their unconditional love and financial support for my two years' master degree studying at Johns Hopkins University.

Without their encouragement, I cannot make great progress on my study here. And thank my friends here at Johns Hopkins University for their companion. Thank my ex-girlfriend Maria Luo for her encouragement and support for helping me survive in the toughest time when I hit rock bottom of my life.

Secondly, many thanks for my advisors, Dr. Martin Pomper and Prof. Honggang Cui, who offers me a great assistance in adapting new life in United States, and as an advisor for helping me advance my research area more into medicine and bioscience from materials science and engineering. Without his guidance and insight, I cannot get a big picture of the whole biomaterials research. Besides, thanks my secondary advisor, Prof. Xing Yang, who currently is a professor at Peking University First Hospital, Department of Nuclear Medicine, for training me on advanced organic synthesis and leading me into the field of molecular imaging. I am grateful for knowing Prof. Martin G. Pomper, who is a pioneer and a well-known professor in nuclear medicine, especially in Prostate Cancer Imaging. His working style and charisma influence me a lot and set a role model for my future.

Third, I want to express my sincere gratitude towards my lab members in Dr. Pomper's lab. First, Thanks Stephanie Slania, who is a third-year PhD student in Biomedical Engineering, for training me on various instruments and equipment on peptide synthesis. Also, she tutors me on various projects in molecular imaging as well. Then, Thanks postdoctoral fellow, Dr. Deepankar

Das, for training me on advanced organic synthesis, making me familiar with all the process on small molecule synthesis. Thanks, Dr. Bei Cheng, for training on *in vitro* study and letting me understand medicinal chemistry better. Last, Thanks Dr. Srikanth Boinapally for offer suggestion on troubleshooting in chemsitry.

Last, Thank Institute for NanoBioTechnology (INBT) for offering me an interdisciplinary research environment by collaborating with various labs from different areas, which set a new research thought for my future scientific studying.

Thank Johns Hopkins University for giving me the opportunity to study in one of the top ten universities in the world, no matter what the future will be, the journey of here would be unforgettable. Thank Chemical and Biomolecular Engineering Department for offering me top-notch research experience and wonderful coursework. Without any help given above, I could not finish the thesis and complete my Master's degree at Johns Hopkins University.

## List of Tables:

<b>Table 1.1</b> Commonly used PET Radionuclides.....	5
<b>Table 1.2</b> Physical properties and decay mode of radiohalogenated element.....	13
<b>Table 1.3</b> Physical properties and decay mode of metal radionuclides .....	14
<b>Table 2.1</b> commonly used radioiodinated radionuclide and applications .....	22
<b>Table 2.1</b> Peptide sequence of the five DP5 targeted peptides.....	28

## List of Figures/scheme:

Figure 1.1. Key steps involving in studying molecular imaging [2] .....	2
Figure 1.2 A simplified small animal PET imaging procedure [2] .....	4
Figure 1.3 Scheme for $^{99m}\text{Tc}$ formation and decay mode [4] .....	6
Figure 1.4 principle and measurement approach for CEST [8] .....	8
Figure 1.5 Classification of CEST contrast agent based on exchange type [9] .....	9
Scheme 1. Synthesis route of [ $^{11}\text{C}$ ]-PIB .....	10
Figure 1.6 standard uptake value of PIB and FDG; PIB retention area [14] .....	10
Figure 1.7 Chemical Structure of [ $^{18}\text{F}$ ]-DCFPyL (left) and [ $^{18}\text{F}$ ]-DCFBC.....	12
Figure 1.8 (a) Axial $^{18}\text{F}$ -DCFBC PET and (b) PET/CT images through the pelvis of prostate cancer patient [15] .....	12
Figure 2.1 Extrinsic and intrinsic pathway of apoptosis [21] .....	18
Figure 2.2. Possible role of TRAIL in neurodegenerative diseases [32] .....	19
Figure 2.3. Chemical structure of prosthetic groups for radioiodination of peptides (I* stands for multiple radioisotopes for iodine).....	24
Figure 2.4. Chemical structure of prosthetic groups for fluorination of peptides.....	25
Figure 2.5. Chemical structure of chelators for the labeling of peptides with $^{99m}\text{Tc}$ .....	26
Figure 2.6. Chemical structures of chelators which is useful for labeling radiometals .....	27
Figure 2.1 FACS analysis of DP peptides for binding to DR5 expressing HCT116 cells.....	31



## **Chapter 1: Chemistry of Molecular Imaging**

### **Background**

Molecular imaging has been emerged as a powerful tool for disease diagnosis on a cellular and molecular level without any interference on its physiological process. Therefore, it is prevalent to use molecular imaging technique to monitor or diagnose disease stage. Based on different imaging mechanism, different imaging techniques have been developed for imaging. Unlike traditional imaging techniques such as CT and MRI which are based on tissue difference, molecular imaging escalates the precision into designing the imaging probe on a molecular level. The ultimate goal of molecular imaging is to localize disease noninvasively and to quantify certain molecular events within living organism <sup>[1]</sup>. What is new for molecular imaging nowadays is that it brings the correlation between molecule and anatomic information. It leads to image-guided molecular therapy and imaging simultaneously. And biomarkers will be utilized to offer imaging and quantification evidence for early disease diagnosis. Molecular imaging is an interdisciplinary topic that involves with multiple subjects such as mathematics, signal processing and chemistry, medicine, etc.

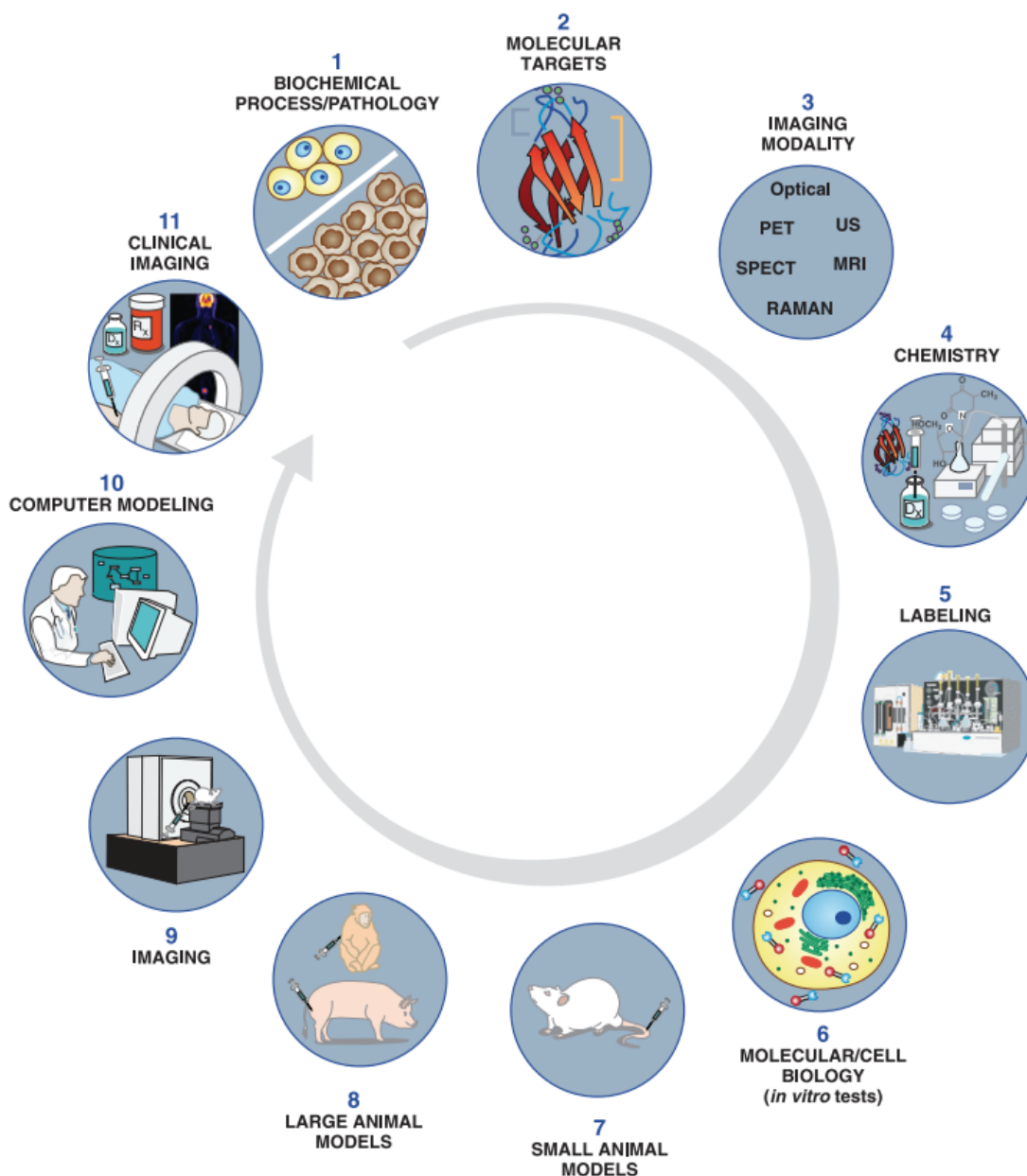


**Figure 1.1.** Key steps involving in studying molecular imaging <sup>[2]</sup>

When applying molecular imaging into disease diagnosis, the first step is to identify a pathological path of interest, and to assess the significance of imaging this process by molecular imaging. The second step is to identify a molecular target that will distinguish itself from other biomarkers which will take a pivotal role in imaging this pathological biochemical process. In this step, a selection of appropriate imaging modalities is also decided. After that, chemists and

radiochemists are working together to design and synthesize the radiotracer to specifically target the biomarker. Then a number of in vitro and in vivo biology-based tests will be conducted to evaluate the imaging agent based on specificity and selectivity. If the radiotracer's final goal is to get FDA approval, it will undergo clinical studies and put it into clinical practice.

## **1.1 Molecular Imaging Techniques**

### **1.1.1 Positron Emission Tomography (PET)**

One of the most commonly used imaging technique which is the most sensitive method in nuclear medicine is Positron Emission Tomography (PET). Positron-emitting radionuclide will be used in this imaging technique, when it decays, two 511keV  $\gamma$ - rays will be produced resulting from the annihilation of the positron emitting from the radionuclide and a surrounding electron in our body. Radionuclides can be incorporated into metabolically active molecules to monitor biological process. When a radionuclide undergoes positron emission decay, the tissue penetration for the positron is ~2mm then they are detected by PET scanner to further process the signal and achieve imaging remodeling [2].

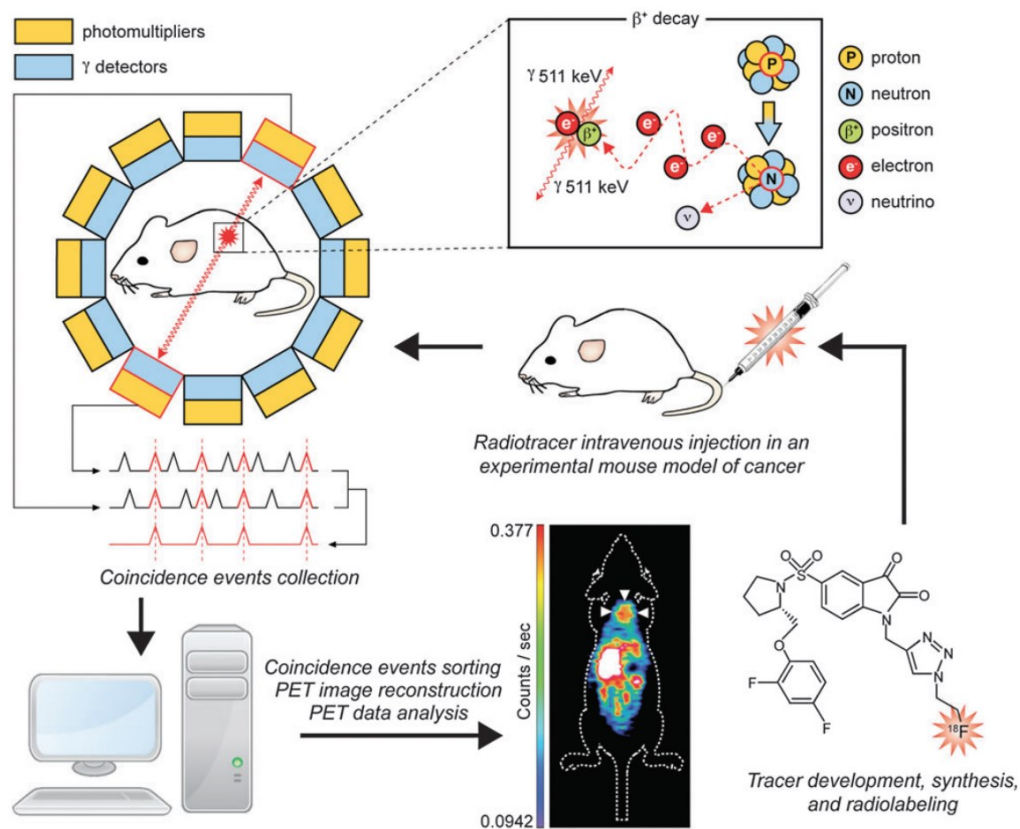


Figure 1.2 A simplified small animal PET imaging procedure [2]

PET possesses high sensitivity which is useful in early disease diagnosis such as cancer and central nervous disease, which will start pathologic change at the cellular level. Radiotracer can take active participation in the physiological process. There are many radioactive tracers to choose from based on their half-lives. When the radiotracer is intravenously injected into the patient and enable effective accumulation before the radionuclide loses its radioactivity.

**Table 1.1** Commonly used PET Radionuclides <sup>[3]</sup>

Nuclide	Half-life (in hour)	Decay Mode
<sup>11</sup> C	0.34	$\beta^+$
<sup>18</sup> F	1.83	$\beta^+$ (97%)
<sup>64</sup> Cu	12.7	$\beta^+$ (18%); $\beta^-$ (37%); EC(24%)
<sup>68</sup> Ga	1.14	$\beta^+$ (89%); EC(17%)
<sup>86</sup> Y	14.7	$\beta^+$ (33%); EC (67%)
<sup>124</sup> I	100.2	$\beta^+$ (23%); EC (77%)
<sup>89</sup> Zr	78.4	$\beta^+$ (23%); EC (77%)

### 1.1.2 Single Photon Emission Computed Tomography (SPECT)

Similar to PET, Single Photon Emission Computed Tomography (SPECT) is another nuclear imaging technique that uses radionuclides as imaging moieties. Unlike PET, the radionuclides for SPECT imaging only involves a single  $\gamma$  ray signal rather than a two way signals based on its decay mode. When a radionuclide decays, apart from generating gamma ray, it also produces alpha and beta radiation. For instance, technetium-99 (<sup>99m</sup>Tc), is a common radionuclide for SPECT imaging. The excited nuclear state is more stable than the average excited states after releasing  $\beta$  particle, therefore the daughter nucleus forms a metastable state, <sup>99m</sup>Tc, which is a nuclear isomer that has a half-life around 6 hours before it transits to <sup>99</sup>Tc, a process that will emit  $\gamma$  ray <sup>[4]</sup>. The other commonly used SPECT radionuclides are iodinated group radioisotopes such as <sup>123</sup>I, <sup>125</sup>I and <sup>131</sup>I.

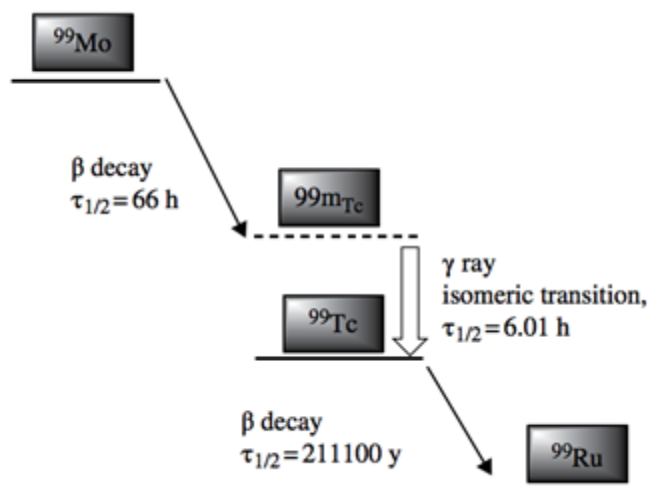


**Figure 1.3** Scheme for  $^{99m}\text{Tc}$  formation and decay mode <sup>[4]</sup>

### 1.1.3 Magnetic Resonance Imaging (MRI)

Magnetic Resonance Imaging (MRI) is a non-invasive imaging technique which is based on nuclear magnetic resonance (NMR) providing anatomical and physiological information on its image. It will give spatial distribution of the intensity of the proton in the body <sup>[5]</sup>, which is a widely used clinical imaging technique. All the proton spins can generate a small magnet charge, when the human body is exposed under the external magnetic field, the protons align with that field. The MRI technicians introduce a radiofrequency pulse which will alter the alignment of protons into 90 degree or 180 degrees. Once the pulse is off, the proton will realign with the magnetic field and release electromagnetic energy along the way. MRI scanner will detect the energy signal and differentiate various tissues in human body.

When we classified the contrast agents, three parameters need to be taken into consideration.

Proton density ( $\rho$ ), longitudinal relaxation time  $T_1$  and transverse relaxation times  $T_2$  and  $T_2^*$  <sup>[6]</sup>.

To better visualize the difference between diseased tissue and normal tissue, contrast agent has been utilized to enhance the imaging contrast after administration into the body. When agents

accumulate, it will increase the relaxation rates of water protons. Other classification category depends on the materials used, based on paramagnetic, superparamagnetic and ferromagnetic materials.

#### **1.1.4 CEST MRI imaging**

Chemical Exchange Saturation Transfer (CEST) contrast agents have paved a new approach to target biomarker through molecular imaging. The difficulties for using MRI technique as an imaging method is tackled by CEST imaging. The inherent low detection sensitivity restricts its contrast agent concentration to around 10  $\mu\text{M}$  – 10mM, therefore the biomarker concentration in vivo is higher than this level. Furthermore, increasing number of researches show that the metallic exogenous contrast agents could alter the cell behavior as well as eliciting cell death <sup>[7]</sup>.

CEST is a relatively new MRI imaging technique which the compounds contain exchangeable protons or exchangeable molecules that can be detected indirectly through water molecules with enhanced sensitivity. The mechanism is very simple: when a radiofrequency (RF) irradiates through exchangeable solute protons which have a different specific frequency resonance than water protons, those exchangeable protons are selectively saturated. Then the saturation is transferred to bulk water when the solute protons exchange with the water protons leading to slight water signal attenuation. In this case, the number of water protons are larger than the number of saturation solute protons. The exchanging process happens repetitively with the unsaturated water protons to prolong the irradiation, allowing the indirect imaging of low concentration solutes represented by water protons signals.

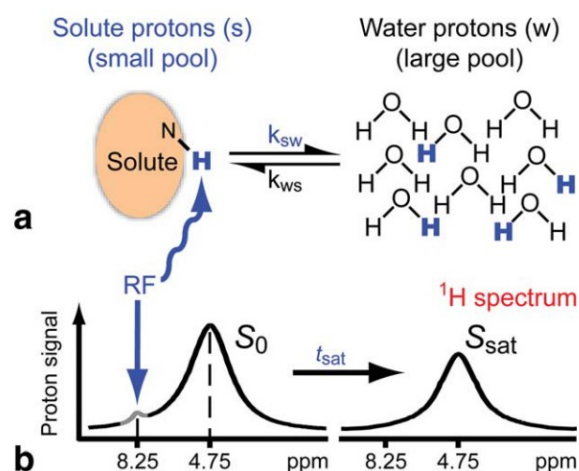


**Figure 1.4** principle and measurement approach for CEST <sup>[8]</sup>

The figure showed above is a simple explanation on the CEST. Amide protons are saturated at specific resonance frequency in the proton spectrum (8.25 ppm), then this saturation is transferred to water (4.75 ppm) at exchange rate  $K_{sw}$ , since the process is a dynamic equilibrium, when the exchange process undergoes a saturation time, the effect becomes visible on water signals like the diagram (b, right).

CEST is the most suitable for molecular and cellular imaging based on different magnetic species from paramagnetic to diamagnetic species, leading to ParaCEST <sup>[9]</sup> and DiaCEST <sup>[10]</sup>. It also can be classified via proton exchange type. First is the proton exchange type, amine, amide and hydroxyl protons and most diamagnetic CEST compounds belong to this group (a). The second is the molecular exchange type. For instance, in a ParaCEST agent, a water molecule coordinated to Europium, this type of molecular exchange is faster than proton-proton exchange (b). The last category is the compartment exchange, as illustrated in the c diagram below, the compartment water and the bulk water difference can result in a single average resonance frequency.



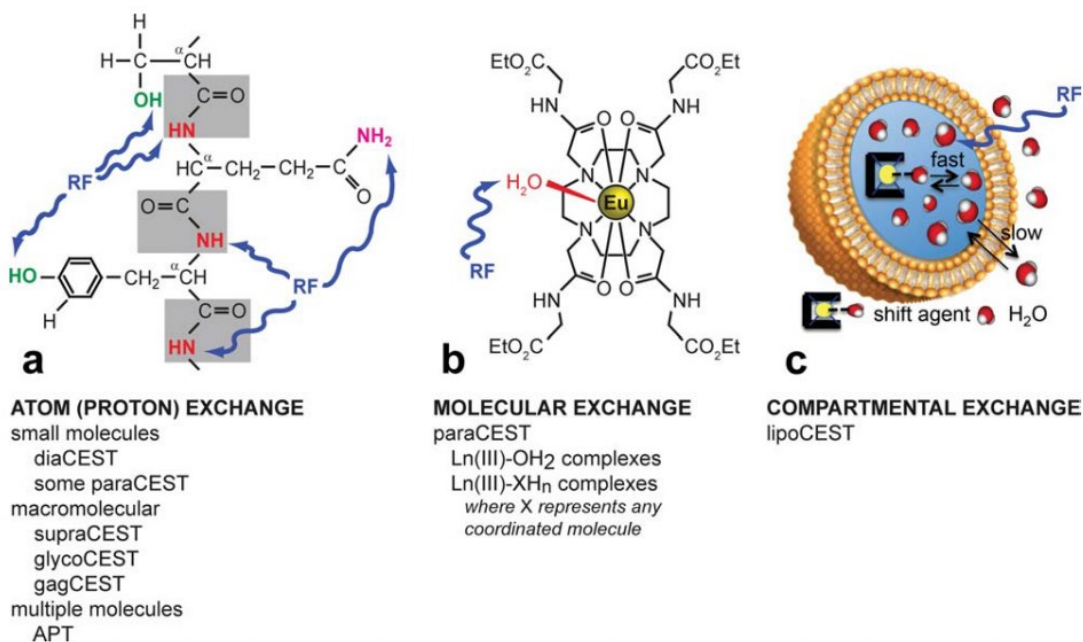


**Figure 1.5** Classification of CEST contrast agent based on exchange type <sup>[9]</sup>

## 1.2 PET/SPECT imaging in Central Nervous Disease

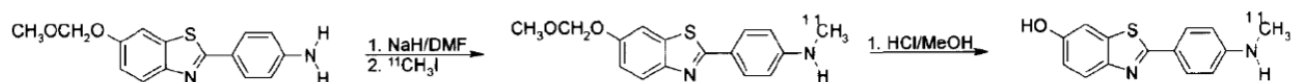
The human brain is the most complex organ which acts as the center of the nervous system. It is very vulnerable to central nervous system (CNS) diseases such as neurodegenerative disorders including Alzheimer's disease (AD), Parkinson's disease (PD) and multiple sclerosis and susceptible to psychiatric conditions including schizophrenia and depression <sup>[10]</sup>. However, studying the brain is not an easy research to conduct.

PET can be used to explore the human brain disorders and diseases. A normal brain needs to consume large quantity of glucose, however, in a pathological brain of AD, the metabolism of glucose as well as oxygen will significantly decrease. 2-deoxy-2-[fluorine-18] fluoro- D-glucose, known as [<sup>18</sup>F] FDG, is a radiofluorinated glucose analog which is widely used in cancer imaging. It is a glucose analog that is closely related to glucose metabolism in various organs. When [<sup>18</sup>F] FDG is taken up by cells, phosphorylated by hexokinase which is highly elevated in

growing malignant tumor cells <sup>[11]</sup>, therefore it's a useful imaging tracer associated with glucose metabolic activity. In central nervous disease, the [<sup>18</sup>F] FDG may be an effective marker to successfully identify the AD and to make early diagnosis with frontotemporal dementia <sup>[12]</sup>.

The difficulty of exogenous imaging tracer to image the brain is limited by a tissue called blood brain barrier (BBB). Blood brain barrier is a highly selective membrane that can separate the circulating blood from brain and extracellular fluid from the central nervous system. It is a tissue formed by brain endothelial cells and only allows water, some gases and lipid-soluble molecules to pass, preventing the neurotoxic materials to get into the brain <sup>[13]</sup>.

One of the most successful PET imaging of amyloid in AD is [<sup>11</sup>C]-PIB, which is the first radiotracer that was put into human trial study. Researchers in university of Pittsburg reports the first human study of amyloid-imaging tracer for Alzheimer's Disease. In this study, AD patients show a marked retention of [<sup>11</sup>C]-PIB in the area of cortex associated with amyloid deposits.



**Scheme 1.** Synthesis route of [<sup>11</sup>C]-PIB

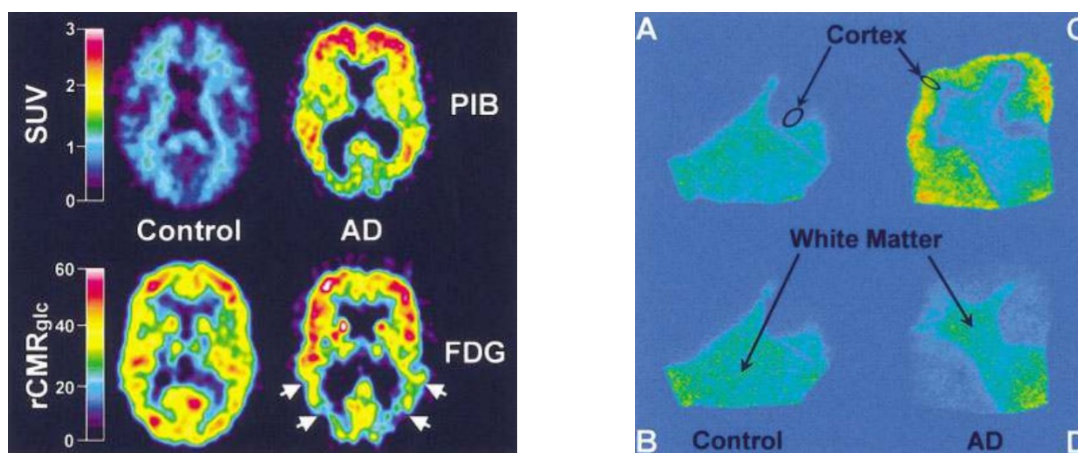


**Figure 1.6** standard uptake value of PIB and FDG; PIB retention area <sup>[14]</sup>

The [ $^{11}\text{C}$ ]-PIB standard uptake value (SUV) clearly illustrates retention compared with the healthy patient. While the healthy patient has FDG retention, high PIB retention in the frontal and temporoparietal cortices of the AD patient <sup>[14]</sup>.

### **1.3 Prostate Specific Membrane Antigen (PSMA) targeted imaging**

Prostate Specific Membrane Antigen (PSMA), also known as glutamate carboxypeptidase II (GCP II), N-acetyl-L-aspartyl-L-glutamate peptidase I or NAAG peptidase, is a type II transmembrane protein with elevated expression on prostate cancer cells. PSMA is the most prostate-specific cell membrane antigen known, which is present in nearly 95% of prostate cancer disease cases. And it will generally increase in expression when prostate cancer progresses. Therefore, it has made itself a useful target for prostate cancer molecular imaging.

The small molecule inhibitor of PSMA is zinc binding compounds attached to a glutamate or glutamate isostere and the most commonly used chemical structure for targeting PSMA is Lys-Glu-urea as targeting scaffold. The most commonly studied PSMA targeting imaging tracer is based on this scaffold with appropriate chemical modification: 1) to improve its binding affinity; 2) to modify its pharmacokinetic properties 3) to chelate radiometals or conjugate prosthetic group onto the radiotracers as imaging moiety. For PSMA-targeting agent, antibodies and small molecules are two types of commonly used imaging agents, which have totally different binding regions of PSMA. The antibody encounter, J591 antibody, on the contrary, binds to an extracellular domain which is distant from the enzymatic pocket. Compared with the current standard imaging of bone scan and CT, PSMA targeted PET/SPECT imaging appears to have higher sensitivity and specificity. Currently, the new PSMA targeted SPECT imaging using

radionuclide such as radiohalogenated group like  $^{18}\text{F}$ ,  $^{123}\text{I}$ ,  $^{124}\text{I}$  or diagnostic radiometals like  $^{68}\text{Ga}$ ,  $^{99\text{m}}\text{Tc}$ ,  $^{64}\text{Cu}$  and therapeutic radiometals such as  $^{177}\text{Lu}$ .  $^{18}\text{F}$ -DCFBC and  $^{18}\text{F}$ -DCFPyL are the two comprehensively studied  $^{18}\text{F}$  PSMA targeted imaging tracers.

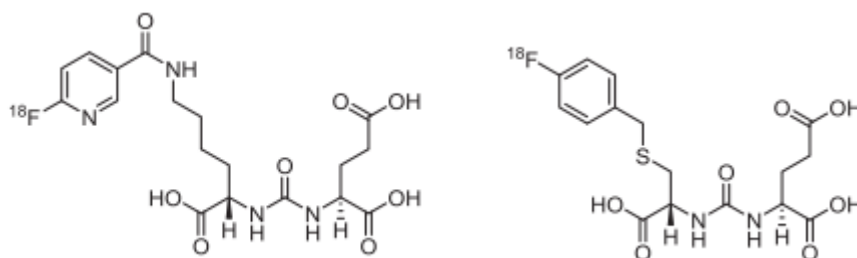


**Figure 1.7** Chemical Structure of  $^{18}\text{F}$ -DCFPyL (left) and  $^{18}\text{F}$ -DCFBC

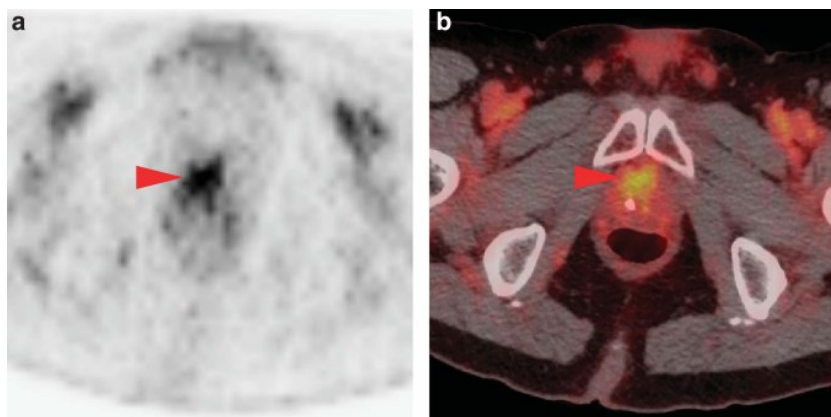


**Figure 1.8** (a) Axial  $^{18}\text{F}$ -DCFBC PET and (b) PET/CT images through the pelvis of prostate cancer patient<sup>[15]</sup>

Apart from radiohalogenated PSMA targeted small molecule inhibitors, radiometal-labeled radiotracers have also been studied. The use of different radionuclide has different function from diagnostic purpose to radiotherapy.  $^{225}\text{Ac}$  and  $^{227}\text{Th}$  are also two radionuclides which have therapeutic value transmitting 97% of their energy through alpha particle emissions.  $^{177}\text{Lu}$  is the beta-emitting radionuclide which has more favorable emission properties and other advantages than previously prevalent studies radionuclides  $^{131}\text{I}$  and  $^{90}\text{Y}$ .

## 1.4. Chemical Methodology for Radiolabeling

### 1.4.1 Halogen Element Radionuclides (F, Br, I)

Halogen group is a crucial element group for radionuclide – fluorine, chlorine, iodine. For the development of PET imaging radiopharmaceuticals,  $^{18}\text{F}$  is considered to be the most ideal radionuclides.  $^{18}\text{F}$  labeled PET imaging has a lower positron energy (0.64MeV) with shorter tissue penetration range (below 2.4 mm) in high specific activity. Moreover, the size of the fluorine atom is similar to hydrogen atom, which makes fluorine a good substitution for hydrogen atom. In the meantime, fluorine is the most electronegative element that can take participate in many reactions.

**Table 1.2** Physical properties and decay mode of radiohalogenated element

Nuclide	half-life (hr)	Decay mode	Maximum Energy of $\beta^+$ (MeV)
$^{18}\text{F}$	1.83	$\beta^+$ , EC	0.635
$^{123}\text{I}$	13.2	EC, $\gamma$	0.159 $\gamma$
$^{124}\text{I}$	100.8	$\beta^+$ , EC, $\gamma$	2.13; $\gamma$
$^{131}\text{I}$	192.8	$\beta^-$ , $\gamma$	0.6 MeV $\beta^-$ ; 0.364 $\gamma$

The most successful approach to prepare high specific activity  $^{18}\text{F}$  radiotracer is based on nucleophilic fluorination reactions. The first category reaction involves the aliphatic nucleophilic substitution ( $\text{S}_{\text{N}}2$ ), while the second category reaction involves the aromatic nucleophilic substitution ( $\text{S}_{\text{N}}\text{Ar}$ ).

### 1.4.2 Metal Radionuclides (Rb, Ga, In, Cu and Tc)

Metal chemistry is another branch to be utilized for molecular imaging, which would enable us to develop new radiotracer based on  $\beta^+$  emitting radiometals. It gains edge over other imaging tracers with easy availability to conjugate biomolecules and ability to form imaging/therapy radiometal pairs. Some important radiometals for developing molecular imaging probes are gallium, indium, yttrium and some transition metals with coordination chemistry. Among the  $\beta^+$  emitting metallic nuclides,  $^{64}\text{Cu}$  ( $T_{1/2} = 12.6$  h),  $^{66}\text{Ga}$  ( $T_{1/2} = 9.45$  h),  $^{86}\text{Y}$  ( $T_{1/2} = 14.74$  h), and  $^{89}\text{Zr}$  ( $T_{1/2} = 3.27$  days) are more appropriate for development of commercial PET radiopharmaceuticals with good transportation advantage. The specific labeling strategies using metal radionuclide will be discussed in further contents.

**Table 1.3** Physical properties and decay mode of metal radionuclides

Nuclide	half-life (hr)	Decay mode	$\beta$ (%) Emission
$^{64}\text{Cu}$	12.8	EC, $\beta^+$ , $\beta^-$	$\beta^+$ (19), $\beta^-$ (40)
$^{66}\text{Ga}$	9.45	EC, $\beta^+$	$\beta^+$ (62)
$^{68}\text{Ga}$	1.14	EC, $\beta^+$	$\beta^+$ (90)
$^{86}\text{Y}$	14.74	EC, $\beta^+$	$\beta^+$ (34)
$^{90}\text{Y}$	64.08	$\beta^-$	$\beta^+$ (93)
$^{89}\text{Zr}$	78.48	EC, $\beta^+$	$\beta^+$ (23)
$^{97}\text{Zr}$	16.8	$\beta^-$ , $\gamma$	$\beta^-$ (100)
$^{111}\text{In}$	67.2	EC, $\gamma$	
$^{99\text{m}}\text{Tc}$	6.01	IT	

### 1.4.3 Organic Radionuclides (C, N, O)

$^{11}\text{C}$ ,  $^{13}\text{N}$  and  $^{15}\text{O}$  are commonly used organic radionuclides for PET imaging tracer development. Carbon, nitrogen and oxygen are major elements in all natural organic molecules where we can

engineer a natural biomolecule into a radiolabeled one. Among the three elements, there is no SPECT radiotracer available for this imaging modality.

$^{11}\text{C}$  is the most successful radionuclide for developing radiotracer because it can be engineered to substitute a stable carbon of a molecule with minimal alteration of its biological properties. However, its short half-life around 20 minutes restricts its application because it requires on site production with cyclotron to prepare the radiotracer.  $[^{11}\text{C}] \text{CO}_2$  is the first radiolabeled compound used to study photosynthesis in plants. After decades of researching, an increasing number of  $^{11}\text{C}$  labeled radiotracers have been developed for clinical studies. The most commonly used organic synthesis labeling strategies for  $^{11}\text{C}$  involves the alkylations of C, N, O and S nucleophiles with  $[^{11}\text{C}]$  methyl iodide or methyl triflate.

## **1.5 Nanoparticles on Molecular Imaging**

Nanoparticles are generally defined as particles with a diameter in the nanometer size range. In biomedical field, nanoparticles can be utilized as carrier, nanomedicine which interacts with cells. However, when the molecular imaging and the nanoparticles are conjugated to radiolabel nanoparticles, the field can be expanded into wide application in theranostics development. The multifunctional nanoparticles possess various function as multimodal imaging and therapy simultaneously <sup>[16]</sup>.

### **1.5.1 Nanoparticles for Magnetic Resonance Imaging (MRI)**

For molecular imaging, the successful contrast agent development should have a high sensitivity. For nanoparticles, there are many ways to control the nanoparticles size, composition and its properties. The sensitivity of MRI can be highly improved by using contrast agent to modify the relaxation time of water protons where nanoparticles can be further incorporated.

The widely studied contrast agents for MRI are paramagnetic gadolinium complexes. It shows great success in detecting breakage of blood brain barrier (BBB), and other lesion or abnormal change in the brain <sup>[17]</sup>. However, the gadolinium-based contrast agent has several limitations such as low relaxivity, high dose injection, short circulation time etc, which may cause side effects <sup>[18]</sup>. Iron oxide-based contrast agents have been furthermore studied since it is safer contrast agent. The iron oxide nanoparticles are mainly cleared by macrophages and degraded in lysosomes which are stored as ferritin and can be used in various biological process in human body <sup>[19]</sup>. Except its good biocompatibility, iron oxide-based contrast agents also have higher sensitivity and easy manipulation of its size, composition <sup>[20]</sup>.

## **Chapter 2: Synthesis, Cyclization and In Vitro Binding Study of Death**

### **Receptor 5 Targeted Peptides**

Cancer is characterized by abnormal cell proliferation and unregulated cell death. Clinically speaking, nowadays the most prevalent way to develop anticancer strategies is to eliminate cancer cell metastasis and induce cell apoptosis <sup>[21]</sup>. Tumor necrosis factor (TNF)-related apoptosis-inducing ligand, known as TRAIL, has a prominent ability to induce apoptosis in malignant cancer cells while pose no harms to majority of untransformed cells, which can be seen as a promising anticancer agent <sup>[22]</sup>. Apoptosis is an inherent and crucial biological process for maintaining cellular homeostasis, dysregulated apoptosis may induce disease such as cancer, autoimmune disorders <sup>[23]</sup>. Tumor necrosis factor-related apoptosis-inducing ligand (TRAIL) is able to bind Death Receptor 4 (DR4) and Death Receptor 5 (DR5), which are promising receptors for cancer imaging. With this promising property, TRAIL has been widely studied for cancer-related therapy and imaging. Apoptosis is a common biological cell death process which is in a genetically regulated form. It is a crucial physiological process that remove unwanted cells



form multicellular organisms <sup>[24]</sup>. Colorectal cancer is one of the most frequently diagnosed cancer in United States, Death Receptor 5 (TRAIL-R2) shows a significant upregulation in colorectal cancer, which can be used as a useful biomarker for colorectal cancer imaging.

## **2.1 TRAIL-induced apoptosis mechanism**

There are two principle routes to the activation of caspases, which the key feature of cell death signaling, namely the intrinsic pathway and the extrinsic pathways <sup>[25]</sup>. Death receptors would utilize the extrinsic pathway to provide death cues to the cells, while the chemotherapeutic agents would trigger the intrinsic pathway. Although there is no well-defined signaling pathways, increasing evidence shows that the two major pathways got a cross-talk <sup>[26]</sup>. TRAIL receptor is not the most powerful target since some tumor cells will use some regulators such as c-FLIP (blocking assembly of DISC), caspase-8, NF- $\kappa$ B, Akt to evade cell death signaling. The extrinsic pathway is activated by ligation of death receptor, adaptor proteins FADD will be recruited to the cytoplasmic tail of the receptor, then recruit procaspases 8/10, assembling into the death-inducing signaling complex (DISC). Next the procaspases 8 and 10 autocatalytically activate themselves. In a series caspase 3, 6, 7 are activated by caspase 9. The extrinsic pathway is independent of p53 activity as well as Bcl-2 or Bcl-xL. The other pathway is intrinsic pathway, which is also called mitochondrial pathway. Unlike extrinsic pathway, intrinsic pathway is activated through activities that is harmful to cells such as cytotoxic agents, cell distress and defective cell cycles, detachment from the extracellular matrix, hypoxia <sup>[27]</sup>. This pathway is triggered by the BCL2 superfamily, engaging a set of proapoptotic Bcl-2 members, the Bax, Bak or Bok to release factors cytochrome c and Smac/DIABLO <sup>[28]</sup>. Within the cytosol, cytochrome c binds APAF1, assembling into an apoptosome that recruits and activates caspase-9, then same as

activation of caspase 3, 6, 7. There is a convergence at both pathways, and clearly p53 appears to be a requirement for initiating death pathway [29].

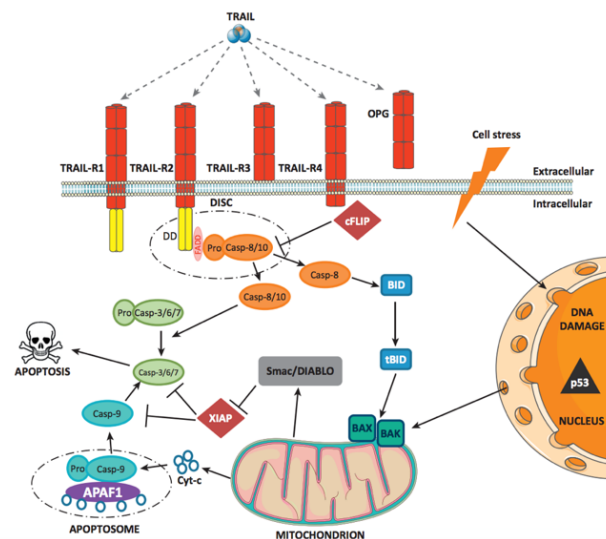


**Figure 2.1** Extrinsic and intrinsic pathway of apoptosis [21]

## 2.2 TRAIL in Liver and Central Nervous Disease

Two other disease has been associated with TRAIL, Liver cirrhosis and neurodegenerative disease have been less focused and the main TRAIL research is on its effect on cancer therapy or imaging. Generally, mature neurons will last the lifespan of the organism [30]. While for neurodegenerative disease, there is an unbalanced cell death, which neuronal cell apoptosis occurs. TRAIL is present in the central nervous system which can induce apoptosis in brain cells. There are studies show that HIV-1-associated dementia, Alzheimer's disease and multiple sclerosis [31].

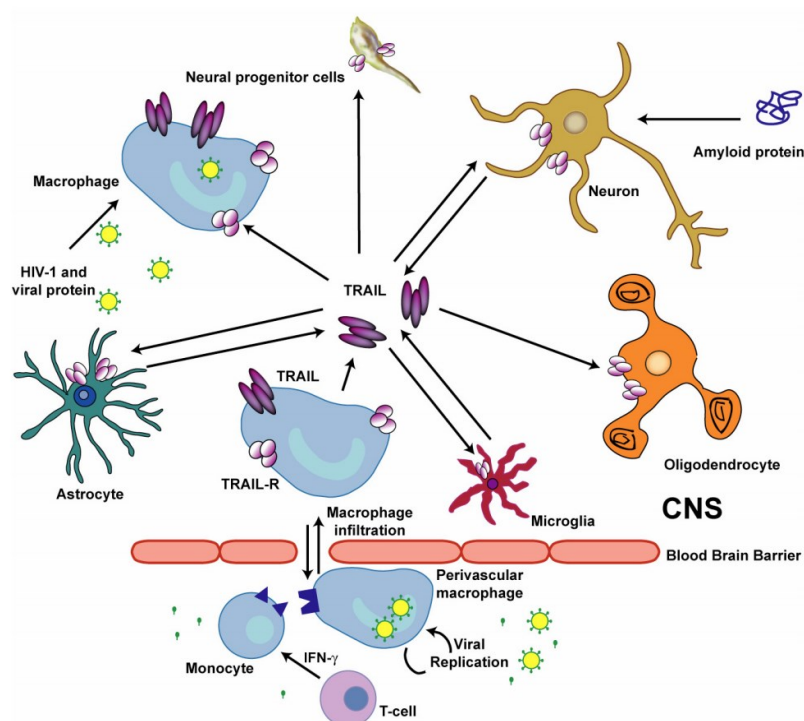


**Figure 2.2.** Possible role of TRAIL in neurodegenerative diseases <sup>[32]</sup>

Liver fibrosis is a common chronic liver disease which will lead to liver cirrhosis and hepatocellular carcinoma, which is a major cause of death. When researchers take a deep look at the liver fibrosis, it has been shown that activated hepatic stellate cells (aHSCs) is the major cells that contribute to the liver fibrosis. Hence the basic strategy to contain liver fibrosis is to preserve quiescent HSCs and eradicate aHSCs. TRAIL, in this case, is an alternative strategy. Studies have shown that aHSCs is associated with an overexpression of death receptors and are sensitive to TRAIL-induced apoptosis. Therefore, Death receptors could be a potential target for actively imaging liver fibrosis and aHSCs apoptosis simultaneously.

### 2.3 Development of DR5-binding peptides using phage display technique

Speaking of types of molecular imaging agents, there are several different categories of them including small molecules, peptides, antibodies, protein fragments and nanoparticles. Due to the size difference of those molecular imaging agents, they have different pharmacokinetic and

binding properties <sup>[33]</sup>. Small molecules and peptides are two classes of molecular imaging agents which are crucial in this study. Small molecules play a significant role in molecular imaging. Its innate advantage of small size make it access to most of the targets from intracellular to CNS targets. And they face less unfavorable biodistribution issues than large molecular weight counterparts. It can cross the biological barriers, clear from the biological system in a relatively short period of time <sup>[34]</sup>. In this project, a library of five phage-displayed peptides has been determined as peptide-based imaging precursor that targets Death Receptor 5 and at the same time, it possesses therapeutic potential to trigger apoptosis.

Solid phase peptide synthesis (SPPS) is a commonly used method to peptide synthesis in a fast and efficient way. A solid support which consists of small, polymeric resin beads functionalized with reactive amine group where peptide chains start to synthesize from C-terminus to N-terminus.

Phage display is a technology that can determine the sequence of high affinity peptide sequence by expressing foreign polypeptides as fusions to capsid proteins which is on the surface of bacteriophage <sup>[35]</sup>. After the screening of combinatorial peptide library against the receptors, the majority of the pharmaceuticals in market is efficacious by selectively interacting with membrane receptors, pharmacologically active small peptide ligands can be discovered with preferable properties than antibodies and proteins.

Biopanning is a common method for obtaining a group of desired peptides from an initial bacteriophage pool. There are three major steps for the affinity selection: 1) introduce phages to an immobilized target; 2) isolate bound and unbound phages by washing; 3) elution of bounded

phages. Generally, in practice, several rounds for selection are necessary for the primary peptides.

## **2.4 Cyclic peptides and cyclization strategies**

Cyclic peptides are peptides chains which formed by linking one end of the peptide structure and other with stable chemical bonds such as amide, disulfide, lactone etc. Various biologically active cyclic peptides are formed in N-to-C cyclization by amide bond formation. Cyclic peptides show better biological activity compared to the linear counterparts because of the conformational rigidity, which means the cyclic peptide has a decreased entropy term of the Gibbs free energy and large surface area for the exposed binding amino acid sequence, therefore it allows enhanced binding affinity towards the target receptor. Also, the structure of the cyclic peptide enables itself resistant to hydrolysis by exopeptidases due to the lack of amino and carboxyl termini. Since the cyclization constrains the flexibility of the peptide structure, it can even be resistant to endopeptidases.

Cysteine (Cys), in this case, is a prevalent constituents of a peptide sequence to form disulfide bonds due to its thiol group on the side chain. A disulfide bond can give peptide higher rigidity and more stability. For instance, peptides are highly prone to metabolic degradation with short biological half-life <sup>[36]</sup>. The disulfide bonds formation is able to prolong its biological half-life by providing higher rigidity.

In this study, iodine oxidation method has been used to cyclize the cysteine residues with ACM protecting group. The iodine oxidation method can remove the ACM group and form disulfide bond at the same time.

## 2.5 Labeling Strategies and Methodologies for Peptides

**Table 2.1** commonly used radioiodinated radionuclide and applications

Radionuclides	Half-life	Application
$^{123}\text{I}$	13.2 h	SPECT imaging
$^{124}\text{I}$	4.2 days	PET imaging
$^{125}\text{I}$	59.4 days	Physiological process in long period (in vivo study)
$^{131}\text{I}$	8.0 days	SPECT imaging & therapy

Peptide radiopharmaceutical is under extensive studying in molecular imaging probe development for recent years. Peptide-based imaging probe is one of the special class of radiopharmaceuticals against small molecules and antibodies with distinct advantages. A lot of research literatures indicate that there are various receptors show high affinity towards both peptides and small molecules ligands. But still peptides are popular in developing imaging probe with the advantages of low molecular weight compared to antibodies, good tissue diffusion and easy chemical modification <sup>[37]</sup>. But when all potential radiopharmaceuticals are evaluated under clinical use, peptide also shows edges over other candidates on clearance kinetics, metabolic stability and easy radiolabeling <sup>[38]</sup>. Peptides are sequences of various amino acids linked together through amide bonds, the side chain of some types of amino acids is chemically active that can be used to radiolabel certain radionuclides. On the contrary, monoclonal antibodies, while it has potential to target tumor, relatively long circulating half-life, its poor tissue penetration loses its advantage over peptide candidates.

There are various radionuclides mentioned above that can be chosen for radiolabeling. In order to design an efficacious radiopharmaceutical, there are some general considerations with respect to the selection of a label. First and foremost, it depends on the application of your radiolabeled compound. Radiopharmaceutical is a special class of drugs, because for imaging purpose, the labeled moiety shows no biological activity. The radionuclides that conjugate to a bioactive biomolecule can alter its properties to hinder an effective binding. An efficacious imaging probe is to demonstrate similar pharmacokinetics, sensitivity and specificity compared to that of non-labeled molecules <sup>[39]</sup> <sup>[40]</sup>.

The half-life of the radionuclides is a crucial consideration for selecting a label. The most desired radionuclide has an appropriate half-life that enables the tracer accumulate in the targeted spot before losing its desired radioactivity. Half-life of undesired radionuclide either is too long or too short. For in vivo study, long half-life radionuclide is not an issue, but for clinical trials, it poses threat on dosing limit. Short half-life radionuclide will lose its optimal radioactivity before it reaches the targeted tissue.

Appropriate labeling methods is also a paramount factor for desired imaging. Different labeling method may have different radio yield and radioactivity. If the tracer will be utilized for clinical use, the high radiolabeling yield must be maintained. On the other hand, if the target tissue expression is low, the radionuclide should have higher specific radioactivity. Another factor that need to be considered is the influence of the labeling method on how it will change the tracer's targeting properties, which will affect the biodistribution.

### 2.5.1 Halogen-labeled peptide radiopharmaceuticals methods

For radioiodination of peptides, there are two general synthetic methods: direct radioiodination by electrophilic substitution and indirect radioiodination by chemical conjugation. Among the various iodine isotopes,  $^{123}\text{I}$ ,  $^{124}\text{I}$ ,  $^{125}\text{I}$  and  $^{131}\text{I}$  are widely used for different imaging modalities.  $^{123}\text{I}$  is a perfect candidate for SPECT imaging,  $\gamma$ -emitting  $^{131}\text{I}$  can be used for SPECT imaging.

For direct radiolabeling of iodine radioisotopes, the labeling target for the peptide is the tyrosine and histidine residues where electrophilic substitution happens in a mild condition. Radioiodide is oxidized to form electrophile  $^*\text{I}^+$  by oxidizing agent such as chloramine T, and N-halosuccinimides. Then  $\sigma$ -complex is formed when  $^*\text{I}^+$  attacks the aromatic rings of tyrosine which is electron-rich. And the hydroxyl group, which is electron-donating, stabilize the  $\sigma$ -complex structure. However, the direct radioiodination is viable only when the peptide has tyrosine and histidine residues. Also, the enzyme tyrosine deiodase will happen when the iodine will be detached and accumulate in the thyroid, which is toxic in vivo.

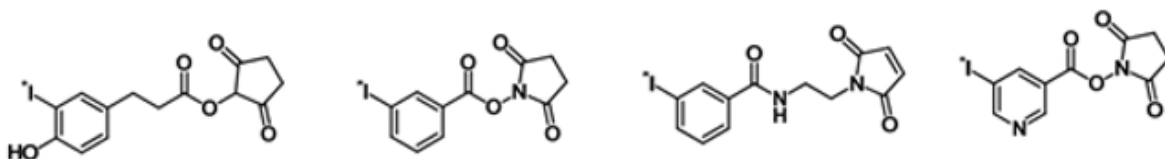


**Figure 2.3.** Chemical structure of prosthetic groups for radioiodination of peptides ( $\text{I}^*$  stands for multiple radioisotopes for iodine)

$^{18}\text{F}$  is a common radionuclide for PET imaging, however, it is impossible to label  $^{18}\text{F}$  onto a molecule in a mild condition via nucleophilic substitution reaction because it is reacted in a high temperature and strong bases condition which will destroy the peptide structure <sup>[40]</sup>.

Prosthetic group is often used for introducing  $^{18}\text{F}$  onto a molecule. First, the  $^{18}\text{F}$  is introduced on



prosthetic group, then simple reaction can link radiolabeled prosthetic group onto the biomolecules by amine, alkyne or azide groups, etc. [ $^{18}\text{F}$ ] SFB and [ $^{18}\text{F}$ ] NPFP are two successful prosthetic groups that use reactive amine group for coupling reaction with good yield and stable biological properties<sup>[40]</sup>. Various [ $^{18}\text{F}$ ] fluorinated prosthetic group reactions are conducted through thiol-maleimide reaction. Chemoselective conjugation methods using aldehydes, alkyne and azide derivatives labeled with  $^{18}\text{F}$  seems more suitable and efficient for clinical applications.

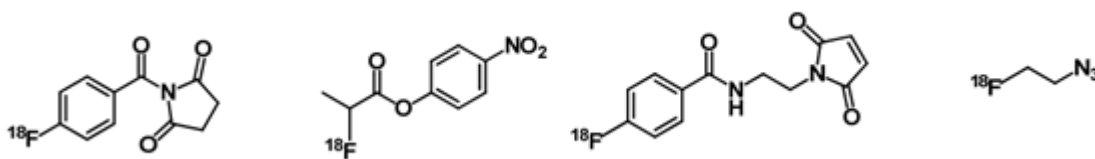


**Figure 2.4.** Chemical structure of prosthetic groups for fluorination of peptides

### 2.5.2 $^{99\text{m}}\text{Tc}$ -labeled peptide radiopharmaceuticals method

$^{99\text{m}}\text{Tc}$  is the most frequently used radionuclide in nuclear medicine with several advantages such as ideal nuclear physical properties, easy commercial availability, low production cost and rich labeling chemistry. Most  $^{99\text{m}}\text{Tc}$  complexes are in the oxidation state of +V, while most  $^{99\text{m}}\text{Tc}$  complexes eluted from the generator are in  $^{99\text{m}}\text{TcO}_4^-$ , a +VII oxidation state. Therefore, reducing agents such as  $\text{Na}_2\text{S}_2\text{O}_4$ ,  $\text{SnCl}_2$  can be used to reduce it to +V oxidation state. The most commonly used strategy is postconjugation strategy, which means a bifunctional chelator is first conjugate to the peptide, then the  $^{99\text{m}}\text{TcO}_4^-$  is reduced with reducing agent and complexed by the chelator.

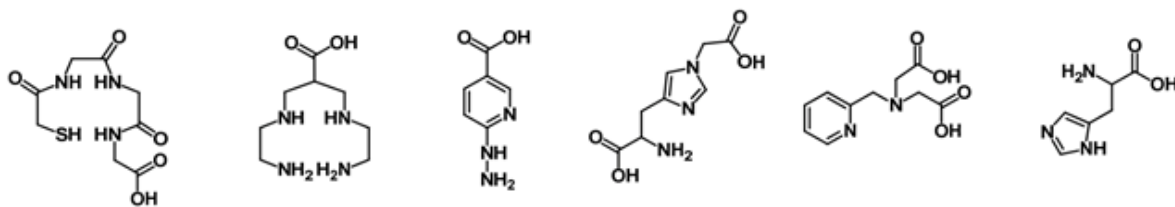


**Figure 2.5.** Chemical structure of chelators for the labeling of peptides with  $^{99m}\text{Tc}$

Another useful strategy is label with the organometallic  $[\text{}^{99m}\text{Tc}(\text{CO}_3)]^+$  core. The  $^{99m}\text{Tc}$  tricarbonyl approach can be used to develop radiopharmaceuticals with the organometallic precursors  $\text{fac-}[\text{}^{99m}\text{Tc}(\text{CO})_3(\text{H}_2\text{O})_3]$ .  $^{99m}\text{Tc}$ -tricarbonyl complexes are formed with a tridentate BFC conjugated peptide, such as (N $\alpha$ -His) Ac or picolylamine diacetic acid (PADA) which show better stability in vivo, compared to mono and bidentate ligands such as histidine [40].

### 2.5.3 Radiometal labeling method

Among the radiometal labeling, radionuclide such as  $^{111}\text{In}$ ,  $^{67/68}\text{Ga}$ ,  $^{86/90}\text{Y}$ ,  $^{177}\text{Lu}$  and  $^{64/67}\text{Cu}$  are the most commonly used radionuclide for peptides. Hard and soft Lewis acids and bases theory, also known as HSAB concept, hard Lewis acids ( $\text{Ga}^{3+}/\text{In}^{3+}$ ) can form thermodynamically stable complexes with hard ligands containing nitrogen and oxygen donor. DTPA is one of the chelators for labeling  $^{111}\text{In}$  with fast labeling kinetics. Another macrocyclic chelator DOTA can be used to chelate divalent and trivalent radiometals such as  $\text{Ga}^{3+}$ ,  $\text{In}^{3+}$ ,  $\text{Y}^{3+}$ ,  $\text{Lu}^{3+}$  and  $\text{Cu}^{2+}$ , which can form thermodynamically and kinetically stable complexes. NOTA is the most favorable chelator for Ga labeling of peptides with higher complex stability than DOTA counterparts due to their cavity size difference. For larger size radiometal ions such as Yttrium, their complexes require higher coordination numbers of 8 or even 9. Due to the favorable pharmacokinetic profiles and appropriate cavity size, DOTA derivatives have been used for the  $^{90}\text{Y}$  and

$^{177}\text{Lu}$  labeling, which forms a more stable complexes than acyclic chelating agents TETA.

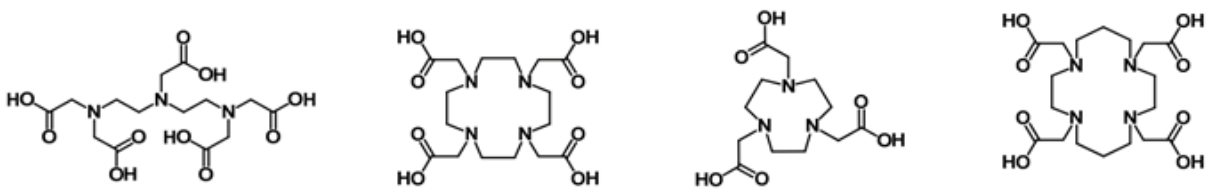


**Figure 2.6.** Chemical structures of chelators which is useful for labeling radiometals

## 2.6 Experimental Section:

**Table 2.1** Peptide sequence of the five DP5 targeted peptides

Peptide ID	Peptide Sequence	Peptide ID	Peptide Sequence
DP1_linear_unlabeled	H <sub>2</sub> N- CVALRKTTC- Ac	DP1_linear_labeled	FAM- CVALRKTTC- Ac
DP2_linear_unlabeled	H <sub>2</sub> N- CGKIRMRTC- Ac	DP2_linear_labeled	FAM- CGKIRMRTC- Ac
DP3_linear_unlabeled	H <sub>2</sub> N- CTKSTMRKC- Ac	DP3_linear_labeled	FAM- CTKSTMRKC- Ac
DP4_linear_unlabeled	H <sub>2</sub> N- CNKPAMKRC- Ac	DP4_linear_labeled	FAM- CNKPAMKRC- Ac
DP5_linear_unlabeled	H <sub>2</sub> N- CYFRFQEEC- Ac	DP5_linear_labeled	FAM- CYFRFQEEC- Ac

In this study, a library of five phage displayed peptides has been determined as peptide-based imaging precursor for Death Receptor 5 and apoptosis simultaneously. The unlabeled linear peptide is prepared for future characterization on its therapeutic potential, the cyclized peptide is prepared to test whether cyclization can enhance the binding affinity and enhanced biological half-life in vivo.

### 2.6.1 Materials and methods:

**2.6.1.1 Materials.** All Fmoc amino acids and cysteine preload Wang resin were purchased from Chem-Impex int'l Inc.. All other reagents such as DMF and TFA were purchased from vwr, honeywell and sigma-aldrich.

**2.6.1.2 DR5 peptide synthesis.** All peptides were synthesized using standard 9-fluorenylmethoxycarbonyl (Fmoc) solid phase synthesis techniques. The peptides were

synthesized on a 0.05 mmol scale using Liberty Blue automated microwave peptide synthesizer (CEM, Matthews, NC, USA). Fmoc deprotection was followed using 20% piperidine in DMF solution for multiple washes. Completed peptides were cleaved from the solid support using a 5 ml mixture of TFA/TIS/H<sub>2</sub>O in a ratio of 95:2.5:2.5 for 3 hrs. Excess TFA was removed by blowing air, the remaining peptide solution was triturated with cold ethyl ether to precipitate the crude peptides, and they were further phase-separated by centrifuge (Megafuge 16, Thermofisher Scientific, Waltham, Massachusetts, USA) in 4500rpm for 5 min, and the ethyl ether was discarded and the rest peptide was air-dried and kept in the vacuum chamber for 3 hours.

**2.6.1.3 Cyclization Reaction.** The cyclic peptide sequence is same compared with the linear one, however, the difference is on the protecting group, for linear peptide, the protecting group for cysteine is trityl (Trt), while for the cyclic peptide, the protecting group is Acetamidomethyl (ACM). The cyclic peptides were cyclized in a filtered-capped syringe. The crude peptides without resin cleavage was transferred to a filter syringe rinsed with 3 ml DMF. Iodine solids were dissolved in 2 ml DMF/H<sub>2</sub>O (ratio of 4:1). The peptides were treated with I<sub>2</sub> solution and shake for 1 hour. After the shaking, separate the resin and solution by filter, then wash the peptide resin with DMF for three times, then wash the peptides with 2% ascorbic acid for three times, wash them with DMF and dichloromethane respectively. The cyclic peptide resins were cleaved using a 5 ml mixture of TFA/TIS/H<sub>2</sub>O in a ratio of 95:2.5:2.5 for 3 hrs. Excess TFA was removed by rotary evaporator, cold ethyl ether was added to precipitate the crude peptides, which were collected and dried under vacuum for 1 hour.

**2.6.1.4 Peptide purification.** All the peptides were purified by preparative RP-HPLC (Agilent Technologies, Santa Clara, CA, USA) equipped with a fraction collector. The separations were preformed using C18 column (Luna, 100 Å, 10 µm, 250×10 mm) at 25°C with monitoring

wavelength at 220 nm. The DP1-4 linear and cyclic peptides were all dissolved in 2 ml 20% acetonitrile in water. A water/acetonitrile gradient of 15% - 80% was run for 30 min containing 0.1% TFA as eluent at a flow rate of 10 ml/min. For DP5 linear and cyclic peptides, they were dissolved in 2 ml 50% acetonitrile in water and separated with a water/acetonitrile gradient of 45% - 80% in 30 min containing 0.1% TFA as eluent with 10 ml/min flow rate. Desired fractions were collected, and then concentrated. Peptides were freeze-dried on lyophilizer (FreeZone - 105°C, Labconco, Kansas City, MO, USA).

The monitored wavelength is 220 nm and the threshold is 200 in a peak based collection mode.

**2.6.1.5 LCMS characterization.** Dissolved the lyophilized peptide in 200  $\mu$ L water, and prepare 50  $\mu$ L of concentrated sample solution to injection vials. The molecular weight of each peptide was characterized by 6120 Quadrupole LC/MS (Agilent Technologies, Santa Clara, CA, USA). All the samples were run in a water/acetonitrile gradient of 10%-90% (containing 0.1% TFA) in 10 min with the flow rate of 0.8 ml/min. No fraction needs to be collected and the desired situation is a single peak in the liquid chromatography diagram to identify molecular mass.

## 2.7 Result and discussion

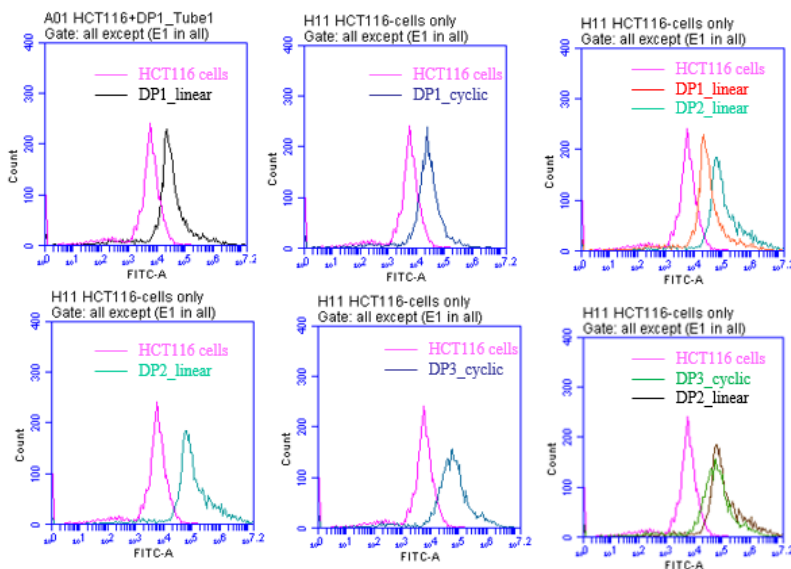


**Figure 2.1** FACS analysis of DP peptides for binding to DR5 expressing HCT116 cells.

The HPLC purification data is listed in Appendices. All the peak above the threshold were collected as potential desired peaks and concentrated for LCMS characterization on its molecular weight. The DP1 to DP4 peptides are highly hydrophilic therefore the retention time is relatively short compared to DP5 peptides based on the gradient of 15%-80% MeCN in 30 min.

As the flow cytometry data indicated above, the formation of disulfide bond has no significant influence on its binding affinity of DP1 peptide. While comparison between DP2 linear peptide and DP1 linear peptide shows that DP2 peptide has better binding affinity than DP1 peptide.

## 2.8 Future perspectives:

In the future, all the five fluorescent-labeled DP linear peptide and cyclic peptide will be synthesized and tested on flow cytometry to compare the binding affinity, then one or two peptides with the highest binding affinity will be screen out for future radiolabeling with DOTA

on chelating radiometals or prosthetic group on  $^{18}\text{F}$  or radioiodinated isotopes such as  $^{125}\text{I}$ . In the meantime, the unlabeled peptide will be used to test its therapeutic potential on whether it has the same biological function to trigger cell apoptosis signal.

### 3. Reference:

- [1] Weissleder, R., & Mahmood, U. (2001). Molecular imaging. *Radiology*, 219(2), 316-333.
- [2] James, M. L., & Gambhir, S. S. (2012). A molecular imaging primer: modalities, imaging agents, and applications. *Physiological reviews*, 92(2), 897-965.
- [3] Vallabhajosula, S. (2009). *Molecular imaging: radiopharmaceuticals for PET and SPECT*. Springer Science & Business Media.
- [4] Long, N. J., & Wong, W. T. (2014). *The chemistry of molecular imaging*.
- [5] Damadian, R. (1971). Tumor detection by nuclear magnetic resonance. *Science*, 171(3976), 1151-1153.
- [6] Caravan, P., Ellison, J. J., McMurry, T. J., & Lauffer, R. B. (1999). Gadolinium (III) chelates as MRI contrast agents: structure, dynamics, and applications. *Chemical reviews*, 99(9), 2293-2352.
- [7] Dua, P., Chaudhari, K. N., Lee, C. H., Chaudhari, N. K., Hong, S. W., Yu, J. S., ... & Lee, D. K. (2011). Evaluation of toxicity and gene expression changes triggered by oxide nanoparticles. *Bulletin of the Korean Chemical Society*, 32(6), 2051-2057.
- [8] van Zijl, P., & Yadav, N. N. (2011). Chemical exchange saturation transfer (CEST): what is in a name and what isn't?. *Magnetic resonance in medicine*, 65(4), 927-948.



- [9] Zhang, S., Merritt, M., Woessner, D. E., Lenkinski, R. E., & Sherry, A. D. (2003). PARACEST agents: modulating MRI contrast via water proton exchange. *Accounts of chemical research*, 36(10), 783-790.
- [10] Zhou, J., & van Zijl, P. C. (2006). Chemical exchange saturation transfer imaging and spectroscopy. *Progress in Nuclear Magnetic Resonance Spectroscopy*, 48(2-3), 109-136.
- [11] PET/SPECT molecular imaging in clinical neuroscience: recent advances in the investigation of CNS diseases. Feng-Mei Lu, Zhen Yuan.
- [12] Bustamante, E., & Pedersen, P. L. (1977). High aerobic glycolysis of rat hepatoma cells in culture: role of mitochondrial hexokinase. *Proceedings of the National Academy of Sciences*, 74(9), 3735-3739.
- [13] Rabinovici, G. D., Rosen, H. J., Alkalay, A., Kornak, J., Furst, A. J., Agarwal, N., ... & Growdon, M. E. (2011). Amyloid vs FDG-PET in the differential diagnosis of AD and FTLD. *Neurology*, 77(23), 2034-2042.
- [14] Klunk, W. E., Engler, H., Nordberg, A., Wang, Y., Blomqvist, G., Holt, D. P., ... & Ausén, B. (2004). Imaging brain amyloid in Alzheimer's disease with Pittsburgh Compound-B. *Annals of neurology*, 55(3), 306-319.
- [15] Rowe, S. P., Gorin, M. A., Allaf, M. E., Pienta, K. J., Tran, P. T., Pomper, M. G., ... & Cho, S. Y. (2016). PET imaging of prostate-specific membrane antigen in prostate cancer: current state of the art and future challenges. *Prostate cancer and prostatic diseases*, 19(3), 223.
- [16] Lee, D. E., Koo, H., Sun, I. C., Ryu, J. H., Kim, K., & Kwon, I. C. (2012). Multifunctional nanoparticles for multimodal imaging and theragnosis. *Chemical Society Reviews*, 41(7), 2656-2672.

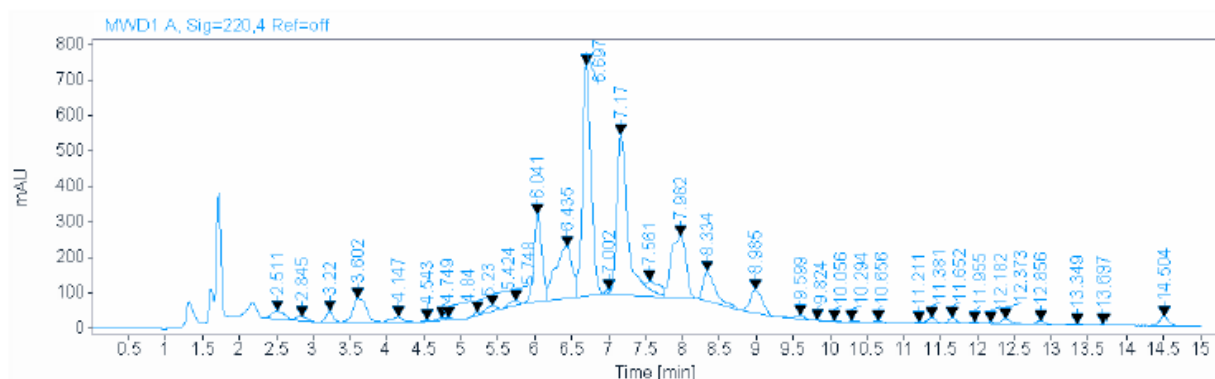
- [17] Yang, C. T., & Chuang, K. H. (2012). Gd (III) chelates for MRI contrast agents: from high relaxivity to “smart”, from blood pool to blood–brain barrier permeable. *Med Chem Comm*, 3(5), 552-565.
- [18] Perazella, M. A. (2009). Current status of gadolinium toxicity in patients with kidney disease. *Clinical Journal of the American Society of Nephrology*, 4(2), 461-469.
- [19] Feliu, N., Docter, D., Heine, M., del Pino, P., Ashraf, S., Kolosnjaj-Tabi, J., ... & Stauber, R. H. (2016). In vivo degeneration and the fate of inorganic nanoparticles. *Chemical Society Reviews*, 45(9), 2440-2457.
- [20] Lee, N., & Hyeon, T. (2012). Designed synthesis of uniformly sized iron oxide nanoparticles for efficient magnetic resonance imaging contrast agents. *Chemical Society Reviews*, 41(7), 2575-2589.
- [21] Stuckey, D. W., & Shah, K. (2013). TRAIL on trial: preclinical advances in cancer therapy. *Trends in molecular medicine*, 19(11), 685-694.
- [22] Vrielink, J., Heins, M. S., Setroikromo, R., Szegezdi, E., Mullally, M. M., Samali, A., & Quax, W. J. (2010). Synthetic constrained peptide selectively binds and antagonizes death receptor 5. *The FEBS journal*, 277(7), 1653-1665.
- [23] Wyllie, A. H., Kerr, J. R., & Currie, A. R. (1980). Cell death: the significance of apoptosis. In *International review of cytology* (Vol. 68, pp. 251-306). Academic Press.

- [24] Nguyen, Q. D., & Aboagye, E. O. (2010). Imaging the life and death of tumors in living subjects: preclinical PET imaging of proliferation and apoptosis. *Integrative Biology*, 2(10), 483-495.
- [25] Ashkenazi, A. (2002). Targeting death and decoy receptors of the tumour-necrosis factor superfamily. *Nature Reviews Cancer*, 2(6), 420.
- [26] Bhojani, M. S., Ross, B. D., & Rehemtulla, A. (2005). TRAIL in cancer therapy. In *Death Receptors in Cancer Therapy* (pp. 263-279). Humana Press.
- [27] Mignotte, B., & Vayssiere, J. L. (1998). Mitochondria and apoptosis. *The FEBS Journal*, 252(1), 1-15.
- [28] Igney, F. H., & Krammer, P. H. (2002). Death and anti-death: tumour resistance to apoptosis. *Nature Reviews Cancer*, 2(4), 277.
- [29] El-Deiry, W. S. (2001). Insights into cancer therapeutic design based on p53 and TRAIL receptor signaling. *Cell death and differentiation*, 8(11), 1066.
- [30] The role of TNF related apoptosis-inducing ligand in neurodegenerative diseases.
- [31] Huang, Y., et al. "The role of TNF related apoptosis-inducing ligand in neurodegenerative diseases." *Cell Mol Immunol* 2.2 (2005): 113-122.
- [32] James, M. L., & Gambhir, S. S. (2012). A molecular imaging primer: modalities, imaging agents, and applications. *Physiological reviews*, 92(2), 897-965.
- [33] Ponto, J. A. (1996). *Handbook of Targeted Delivery of Imaging Agents*.
- [34] M. Werle, A. Bernkop-Schnürch, *Amino Acids* 2006, 30, 351– 367.

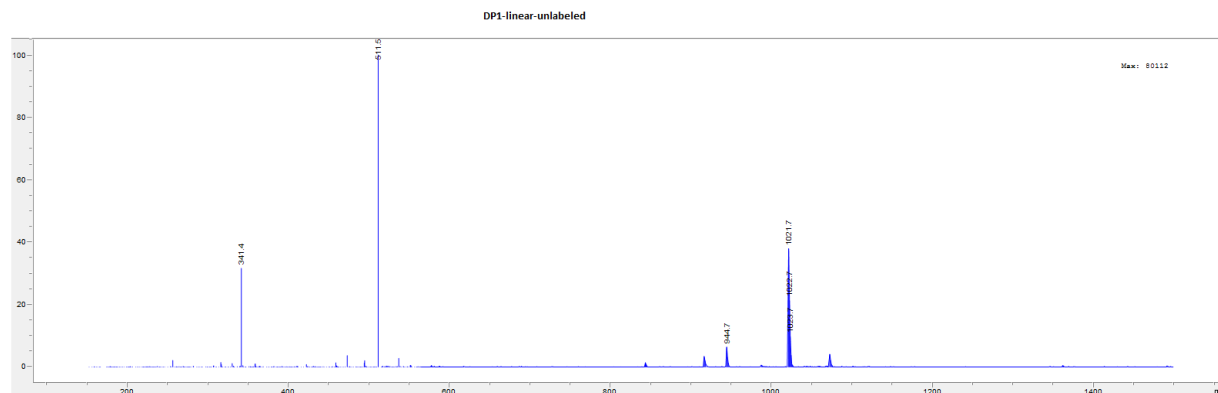
- [35] Smith G.P. Filamentous fusion phage: novel expression vectors that display cloned antigens on the virion surface. *Science* 1985, 228, 1315-1317
- [36] Peptide-based probe for cancer imaging. *J Nucl Med* 2008; 49: 1735 - 1738
- [37] Molecular imaging targeting peptide receptors. *Methods* 48 (2009) 161 – 177
- [38] radiolabeled proteins for positron emission tomography: Pros and cons of labeling methods. *Biochimica et Biophysica Acta* 1800 (2010) 487-510
- [39] pharmacokinetics of internally labeled monoclonal antibodies as a gold standard: comparison of biodistribution of  $^{75}\text{Se}$ ,  $^{111}\text{In}$ , and  $^{125}\text{I}$ -labeled monoclonal antibodies in osteogenic sarcoma xenografts in nude mice.
- [40] Synthesis of peptide radiopharmaceuticals for the therapy and diagnosis of tumor diseases. *Molecules* 2013, 18, 3379-3409

## 4. Appendices

### Appendix 1: HPLC chromatogram and Mass Spectra of DP1 linear unlabeled peptide

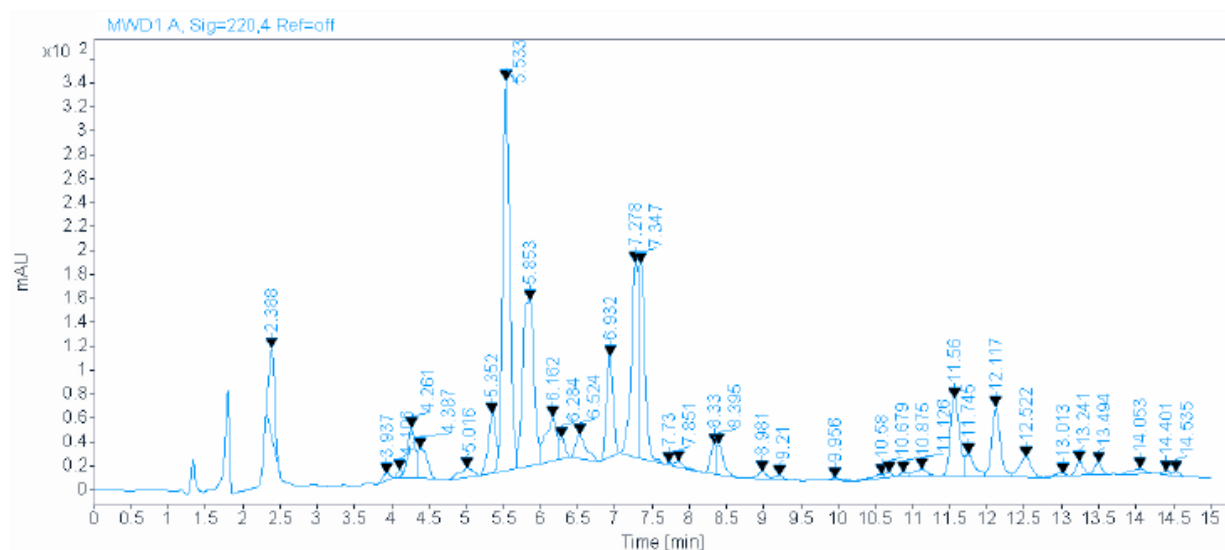


Purification gradient: A water/acetonitrile gradient of 15% - 80% was run for 30 min containing 0.1% TFA as eluent at a flow rate of 10 ml/min.

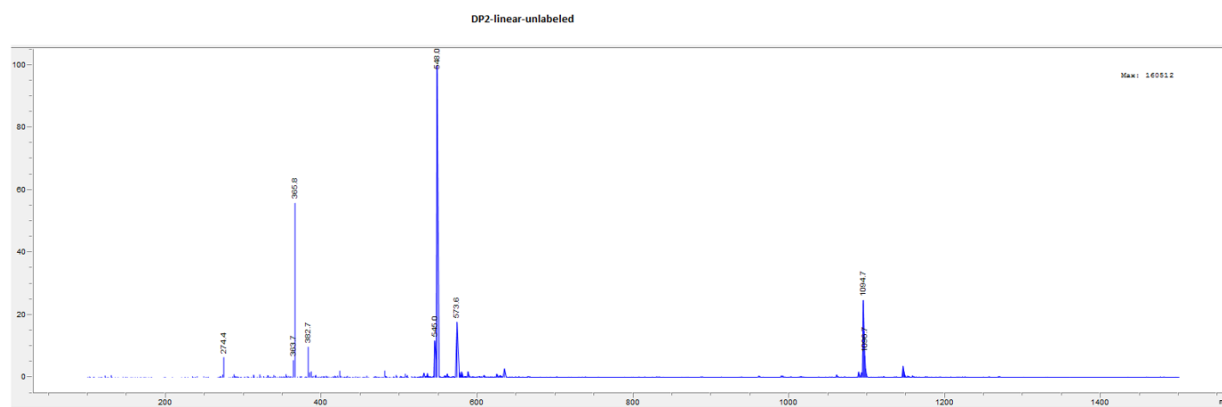


The mass spectrum indicates a base peak at m/z 511.5 assuming the peptide ions are most abundant in the 2+ charge state, and protonated  $[M+H]^+$ , the peak of  $[C_{42}H_{81}N_{14}O_{11}S_2]^+$  peak with mass of 1022.7 is observed. The DP1 linear unlabeled peptide has purity over 90%.

## Appendix 2: HPLC chromatogram and Mass Spectra of DP2 linear unlabeled peptide

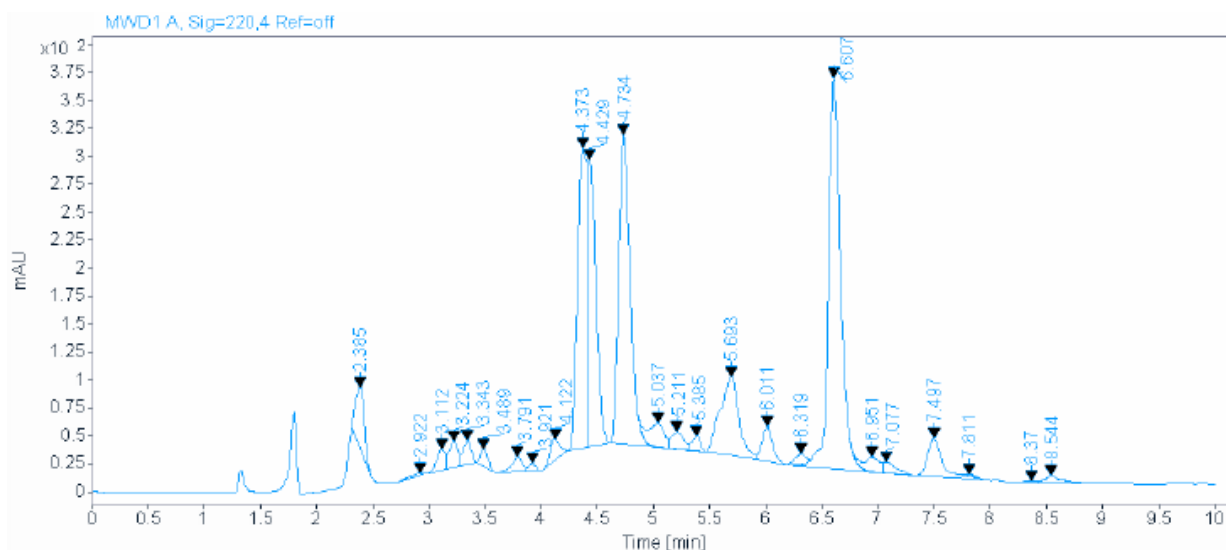


Purification gradient: A water/acetonitrile gradient of 15% - 80% was run for 30 min containing 0.1% TFA as eluent at a flow rate of 10 ml/min.

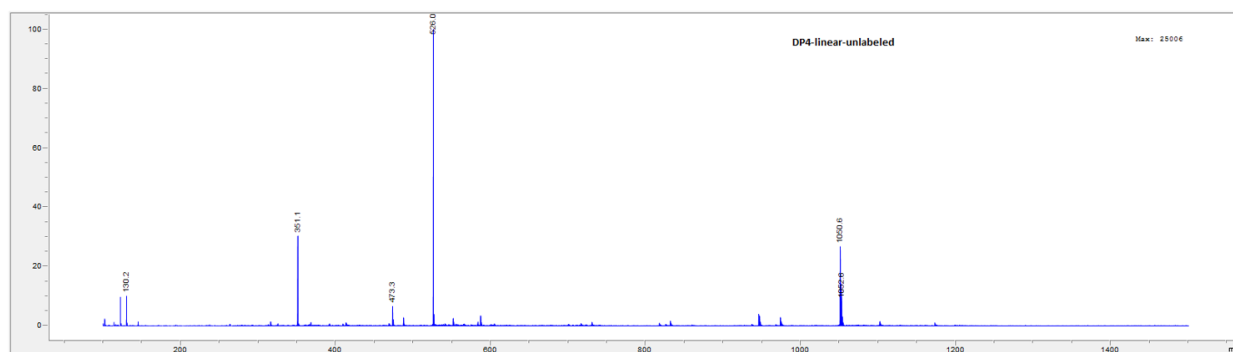


The mass spectrum indicates a base peak at  $m/z$  548.0 assuming the peptide ions are most abundant in the 2+ charge state, and protonated  $[M+H]^+$ , the peak of  $[C_{43}H_{84}N_{17}O_{10}S_3]^+$  peak with mass of 1094.7 is observed. The DP2 linear unlabeled peptide has purity over 90%.

### Appendix 3: HPLC chromatogram and Mass Spectra of DP4 linear unlabeled peptide

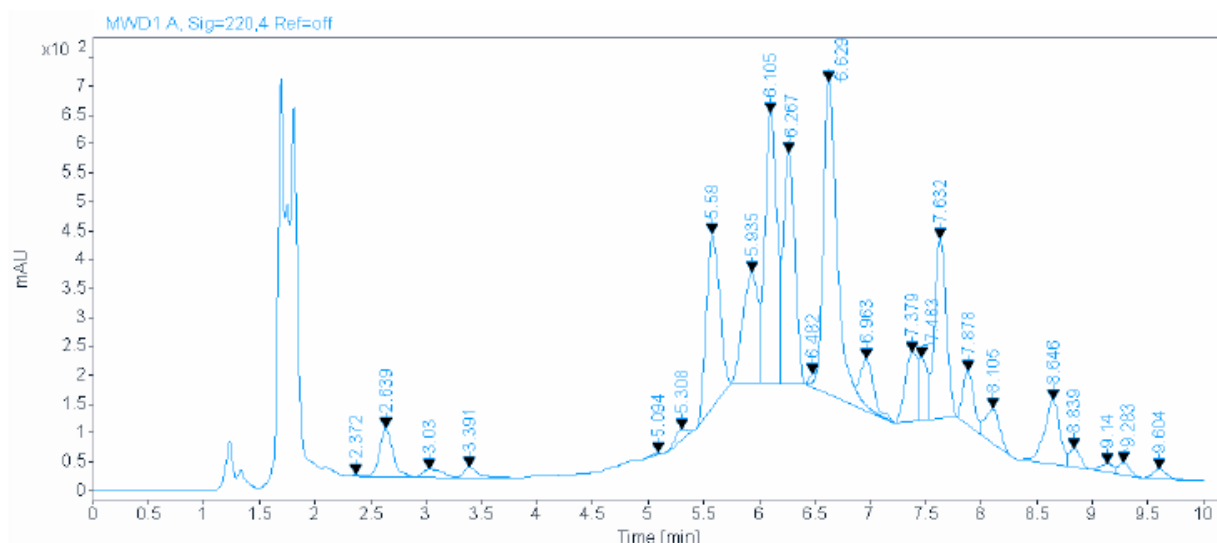


Purification gradient: A water/acetonitrile gradient of 15% - 80% was run for 30 min containing 0.1% TFA as eluent at a flow rate of 10 ml/min.

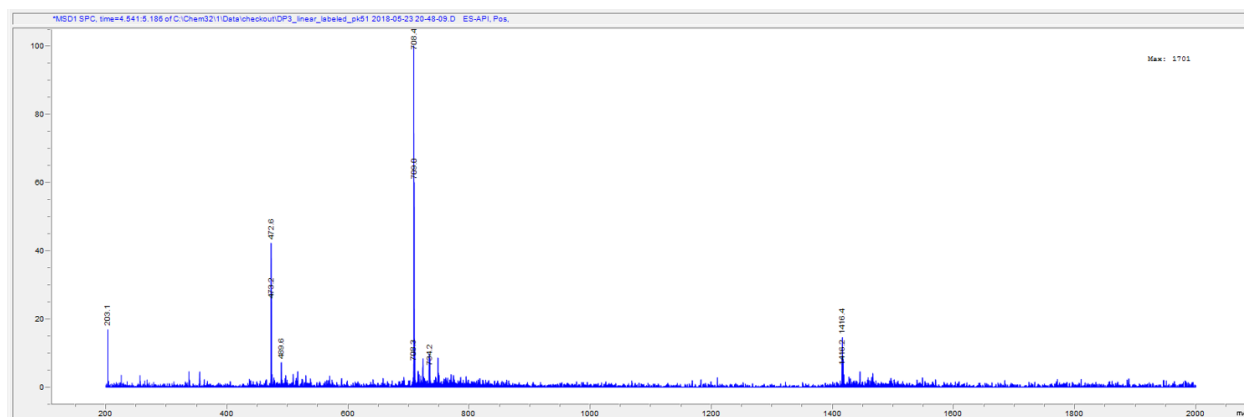


The mass spectrum indicates a base peak at m/z 526.0 assuming the peptide ions are most abundant in the 2+ charge state, and protonated  $[M+H]^+$ , the peak of  $[C_{41}H_{76}N_{15}O_{11}S_3]^+$  peak with mass of 1050.6 is observed. The DP4 linear unlabeled peptide has purity over 90%.

#### Appendix 4: HPLC chromatogram and Mass Spectra of DP3 linear labeled peptide



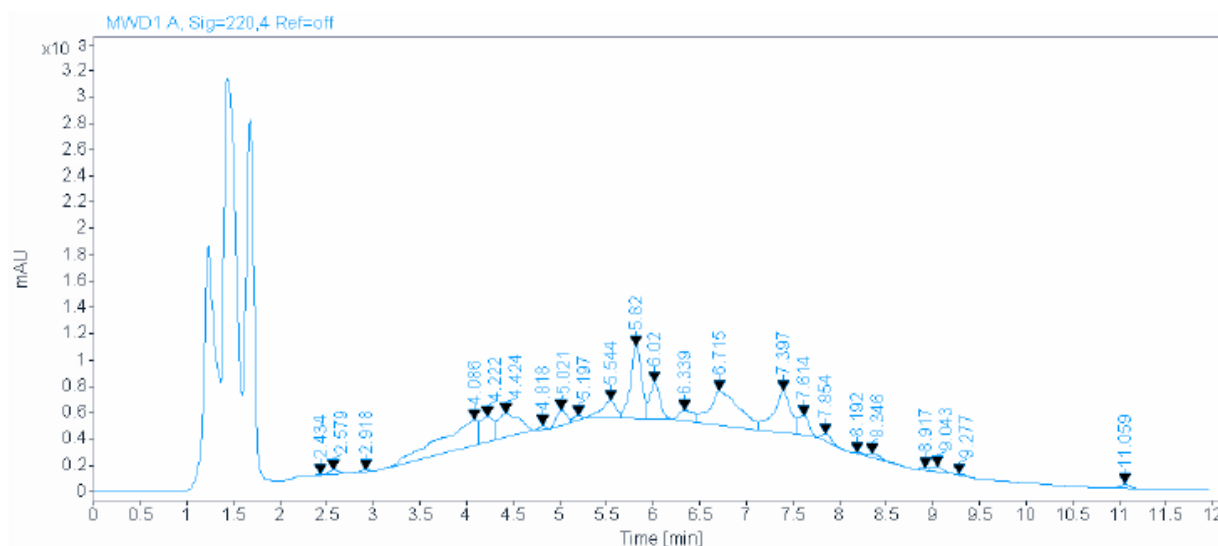
Purification gradient: A water/acetonitrile gradient of 15% - 80% was run for 30 min containing 0.1% TFA as eluent at a flow rate of 10 ml/min.



The mass spectrum indicates a base peak at  $m/z$  708.4 assuming the peptide ions are most abundant in the 2+ charge state, and protonated  $[M+H]^+$  with mass of 1416.4 is observed. The DP3 labeled peptide has purity over 90%.

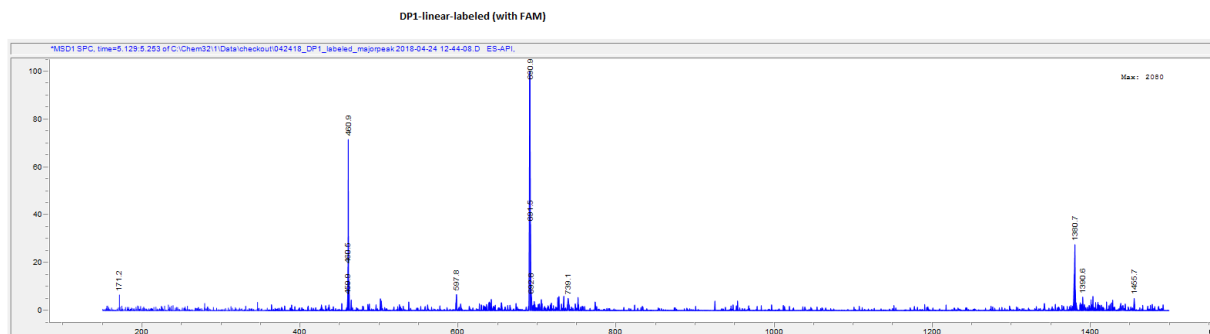


## Appendix 5: HPLC chromatogram of DP3 cyclic labeled peptide



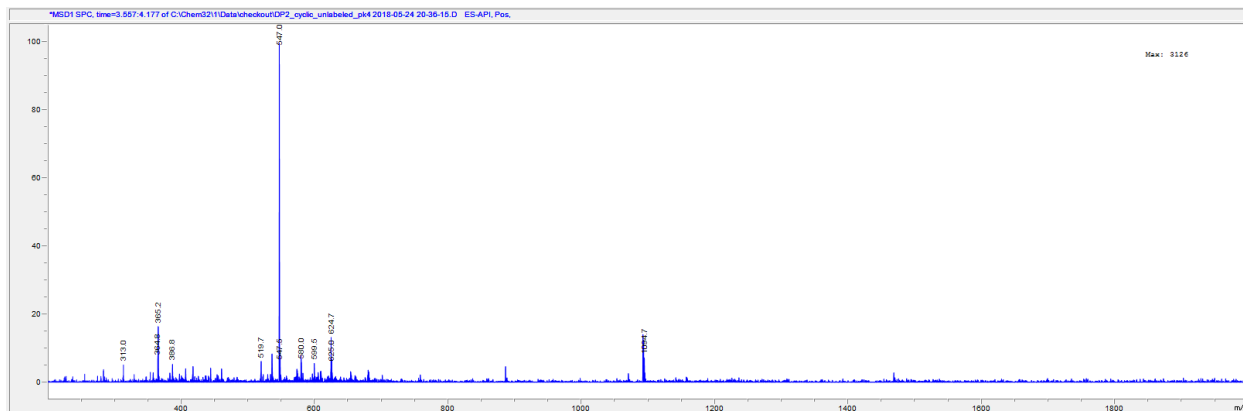
Purification gradient: A water/acetonitrile gradient of 15% - 80% was run for 30 min containing 0.1% TFA as eluent at a flow rate of 10 ml/min.

## Appendix 4: Mass Spectra of DP1 linear labeled peptide



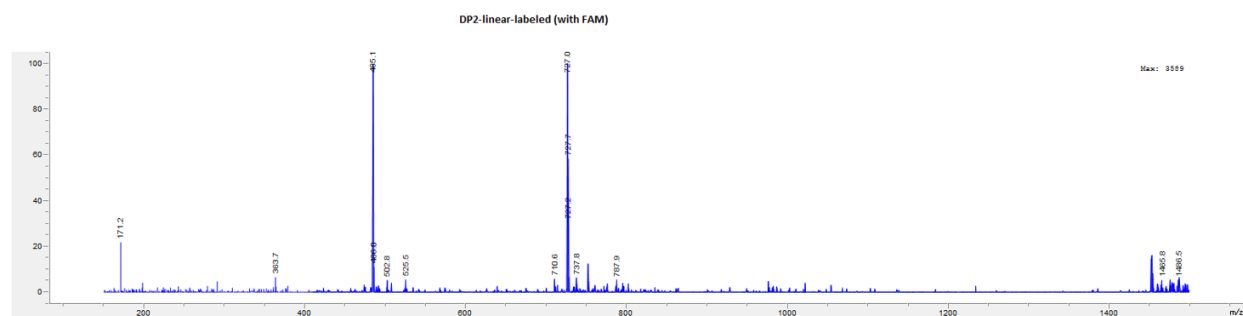
The mass spectrum indicates a base peak at m/z 690.9 assuming the peptide ions are most abundant in the 2+ charge state, and protonated  $[M+H]^+$  with mass of 1380.7 is observed. The DP1 linear labeled peptide has purity over 90%.

## Appendix 5: Mass Spectra of DP2 cyclic unlabeled peptide



The mass spectrum indicates a base peak at  $m/z$  547.0 assuming the peptide ions are most abundant in the 2+ charge state, and protonated  $[M+H]^+$  with mass of 1094.7 is observed. The DP2 cyclic unlabeled peptide has purity over 90%.

## Appendix 6: Mass Spectra of DP2 linear labeled peptide



The mass spectrum indicates a base peak at  $m/z$  727.7 and 485.1 assuming the peptide ions are abundant in the 2+ charge state and +3 charge state. The DP2 linear labeled peptide has purity over 90%.

## **Li, Chenyang**

3300 N Charles St, Baltimore, United States 21218

+1 4109000951 | cli91@jhu.edu

### **EDUCATION**

---

#### **Master of Science in Engineering : Johns Hopkins University**

Baltimore, MD,

United states

- Chemical and Biomolecular Engineering (ChemBE)

Aug. 2016-

Current

#### **Bachelor of Engineering: Beijing University of Chemical Technology**

Beijing, China

- Biofunctional Materials, College of Materials Science and Engineering (MSE)

Sep.2012-Jun.2016

- GPA: 3.51/4.0     Junior GPA: 3.84/4.0

### **PRACTICAL EXPERIENCE**

---

#### **Research participant in Johns Hopkins University**

October 2016 – now

- Under the supervision of Prof. Xing Yang, who is an assistant professor in the Russel H. Morgan Department of Radiology in Johns Hopkins School of Medicine. The main research we undergo is the study of different small molecules inhibitors of Prostate-Specific Membrane Antigen (PSMA) and its application on the Prostate cancer (PCa) imaging at different stages. Also, multiple overexpressed membrane-bound receptors like CAIX and DR5 are investigated for the biomarker of oncology imaging. Currently working (from October 2016 - now) in one of the division of Dr. Martin Pomper's lab in Homewood Campus. The major duty is to help researchers to synthesize the peptide and HPLC purification for further biological research on binding affinity and imaging like PET/SPECT oncology imaging.

## **Synthesis & Characterization of Calcium Carbonate Vaterite Microspheres in different Solution**

Feb.2015- July.2015

- Chemicals co-precipitation method: magnetically stirred under 1800 rpm
- Glycine was used as additives in inducing vaterite  $\text{CaCO}_3$
- The optimum concentration of the formation of the vaterite was learned by setting different glycine concentration magnitude
- To save the vaterite preparation time, experiment on crystallization kinetics were carried by measuring the conductance by electric conductometer
- Malonic acid was added to study the influence of numbers of carboxyl groups on the formation of vaterite microspheres; polyvinyl pyrrolidone(PVP)/sodium dodecyl sulfonate(SDS) were mixed to regulate the morphology of calcium carbonate

## **Preparation and Properties of Chitosan/Sodium Lignosulfonate Microcapsules Formulated by Layer-by-Layer Self-Assembly Using Calcium Carbonate as Sacrificial Templates**

Feb.2015- Current

*Research group leader*

- vaterite  $\text{CaCO}_3$  microspheres were prepared and used as templates for L-b-L self-assembly process. Different methods were tried and the results were characterized by SEM
- The microcapsules were prepared by layer-by-layer polyelectrolytes self-assembly using chitosan and sodium lignosulfonate as shell materials
- Alternate Adsorption (8-10 layers) of polyelectrolytes Chitosan/lignosulfonate through electrostatic attraction to further assemble the calcium carbonate, then the  $\text{CaCO}_3$  was dissolved with EDTA to form hollow microcapsules
- Each assemble process has been sampled and then analyzed by zetasizer to measure  $\zeta$ (zeta) potential
- Currently solving the problem of how to firm the electrostatic adherence of chitosan and lignosulfonate, how to guarantee the evenly distributed microcapsules in solution and prevent the formation of agglomerates

## **Scientific and English Technical Report Contest: Introduction on Gene Delivery**

Fall 2014

- Video Clips: [http://v.youku.com/v\\_show/id\\_XMTQyMTc2NTQ4NA==.html](http://v.youku.com/v_show/id_XMTQyMTc2NTQ4NA==.html)
- First prize, Scientific and Technical Report Contest for Introduction to Material, BUCT
- The Lecture provides a brief overview on the concept and the aim of gene delivery, the gene delivery systems and use of different materials as a carrier in the area of gene therapy.
- Mechanism on DNA complexation is briefly introduced: the amine group( $-NH_2$ ) can be sustained as  $NH_2^+$  under physiological conditions to bind DNA by static attraction which is negatively charged due to phosphate group
- Mechanism on DNA delivery is learned: the DNA complex undergoes cellular uptake via endocytosis, the DNA is released into nucleus for further gene expression
- Lipid-based vectors, cyclodextrin-based vectors and cationic polymeric vectors are introduced respectively: some typical and frequently used materials like poly(L-lysine), polyethylenimine(PEI), poly[2-(dimethylamino) ethyl methacrylate] (PDMAEMA)
- Basic characterization methods related to Gene Delivery are well understood

## **Bachelor's thesis: Synthesis of 2D MoS<sub>2</sub>-peptide nanohybrid materials and study of its application**

Dec. 2015- Graduation

- Two-Solvent Grinding-assisted Liquid phase exfoliation method is used to exfoliate bulk MoS<sub>2</sub> into few layered 2D MoS<sub>2</sub> nanoflakes: N-methyl-2-pyrrolidone (NMP) and ethanol were used to exfoliate MoS<sub>2</sub> bulk materials
- Ionic Liquid BMIMPF<sub>6</sub> (IL) is used as solvent to assist exfoliation process
- Synthesis of self-assembled peptide nanofibers (sequence: RGDAEAKAEAKAEAKAEAKCCY)
- During the exfoliation, there are defects on the surface of 2D MoS<sub>2</sub> layers, using thiol chemistry to functionalize the MoS<sub>2</sub>.
- Characterization of 2D MoS<sub>2</sub> nanoflakes by TEM, HRTEM, AFM
- Characterization of properties: UV-vis spectra, photoluminescence of 2D MoS<sub>2</sub> nanoflakes

### **Lab Training on Biomaterials**

- Acylation of Gelatin and preparation of enteric microcapsules
- Preparation and characterization of microcapsules by w1/o/w2 double emulsion method
- Lab training on cell culture
- preparation of pre-adsorption of PNIPAM on polystyrene(PS) microsphere and study of its effect on non-specific protein adsorption of lysozyme
- specific local test of blood coagulation of materials surface by coagulometers: prothrombin time(PT) and Activated partial thromboplastin time(APTT) are tested
- Polymerization of UV curable resin

### **Study of the Application of Polyurethane in Biomaterials**

Spring 2014

- Conducted synthesis experimentation of polyurethane
- Weissenberg effect was observed; improved hands on ability in chemical experiment
- Became acquainted with polymer physics and polymer chemistry

### **SKILL & INTERESTS**

- Technical Skills: proficient in C, Origin, Chemoffice, Excel, Word, PowerPoint, Photoshop, etc.;
- Interests: Music, basketball, badminton, table tennis, travel